UNIVERSITY OF UDINE
DEPARTMENT OF MEDICAL AND BIOLOGICAL SCIENCES

PhD COURSE IN
BIOMEDICAL AND BIOTECHNOLOGICAL SCIENCES
XXV CYCLE

ENERGETICS AND MECHANICS OF RUNNING: THE INFLUENCE OF BODY MASS AND THE USE OF RUNNING SPECIFIC PROSTHESES

Supervisors
Prof. Pietro Enrico di Prampero
Prof. Rodger Kram

PhD Student
Paolo Taboga

ACADEMIC YEAR 2012-2013

ABSTRACT

The first measurements on running humans date back since the beginning of 20th century (see for example figure 1.1). However, most of the studies were focused on ordinary/average subjects. To better understand how body characteristics influence the biomechanics and the energetics of running, extra-ordinary subjects and athletes need to be involved. This thesis will be divided in two main parts: the first part will focus on the influence of body mass on the energetics and biomechanics of running; the second part will focus on the use of running specific prostheses in sprint running.

PART I. In the first part we investigated the relationship between mechanical and energy cost of transport and body mass in running humans. Ten severely obese (body mass ranging from 108.5 to 172.0 kg) and 15 normal-weighted (52.0–89.0 kg) boys and men, aged 16.0–45.8 years, participated in this study. The rate of O_2 consumption was measured and the subjects were filmed with four cameras for kinematic analysis, while running on a treadmill at 8 km $\cdot$ h^{-1}. Mass specific energy cost (C_r) and external mechanical work (W_{ext}) per unit distance were calculated and expressed in joules per kilogram per meter, efficiency (η) was then calculated as $W_{ext} \times Cr^{-1} \times 100$. Both mass-specific C_r and W_{ext} were found to be independent of body mass (M) (C_r = 0.002 M + 3.729, n = 25, R^2 = 0.05; W_{ext} = -0.001 M + 1.963, n = 25, R^2 = 0.01). It necessarily follows that the efficiency is also independent of M (η = -0.062 M + 53.3298, n = 25, R^2 = 0.05). The results strongly suggest that the elastic tissues of obese subjects can adapt (e.g., thickening) to the increased mass of the body thus maintaining their ability to store elastic energy, at least at 8 km $\cdot$ h^{-1}speed, at the same level as the normal-weighted subjects.

PART II. In the second part we investigated two aspects of sprint running: the start, in particular starting blocks configurations, and curve running.

Part IIa: The aim of the present study was to measure the effect of starting block configuration on starting performance of both non-amputee sprinters and athletes with unilateral transtibial amputations. A total of 16 subjects participated in this study: 7 (6 males and 1 female) were non-amputee sprinters and 9 (7 males and 2 females) were sprinters with a unilateral transtibial amputation. Each subject performed a total of 6 starts, alternating between their usual and unusual starting block configurations, on two separate force platforms located underneath a runway covered with a rubber mat, which allowed each athlete to use their own spiked shoes. For each amputee sprinter, we used data from their unaffected leg (UL) and affected leg (AL) to simulate their start mechanics as if they had two unaffected legs ("a virtual non-amputee") or had two affected legs ("a virtual bilateral amputee"). Non-amputee sprinters had better horizontal acceleration, and therefore overall better starts, in their usual configuration (7.63 ± 0.91 vs. 7.39 ± 0.84 $m \cdot s^{-2}$, p=0.042, n=7). When amputees put their UL on the front block, they developed 6% greater mean resultant forces (1.38 ± 0.06 vs. 1.30 ± 0.11 BW, p=0.015, n=9). However, in contrast with our hypothesis, horizontal acceleration was not statistically different between the UL and AL in front configurations. Virtual bilateral amputee sprinters had worse start performance compared to virtual non-amputees: a 21% smaller resultant force and a 6% more vertical push-angle (although not statistically different), which resulted in a 23% slower horizontal acceleration. These results support the impression that, among similar-level athletes (i.e. same overall times), bilateral amputees have slower starts than unilateral amputees, and unilateral amputees have slower starts than non-amputees.

Part IIb: The first objective of this study was to compare curve running performance between non-amputee sprinters and sprinters with unilateral transtibial amputations. We hypothesized that athletes with and without unilateral transtibial amputations would be slower during maximal speed curve

running compared to maximal speed straight running. Given that the inside leg is thought to limit curve running speed, we hypothesized that sprinters with a unilateral leg amputation would be slower in curves with their affected leg on the inside of the curve, compared to curves with their affected leg on the outside of the curve.

A total of 14 subjects participated: 6 (5M/1F) non-amputee sprinters, 6 (5M/1F) sprinters with a right leg transtibial amputation, and 2 (1M/1F) sprinters with a left leg transtibial amputation. Each subject performed a total of six 40 m sprints on a standard synthetic track surface, wearing their own spiked shoes. The curve of the track was not banked and had a radius of 17.2 m. Each subject performed two sprints in a straight direction (S), two on a clockwise (CW) curve and two on a counterclockwise (CCW) curve. We used a high-speed video camera with a frame-rate of 210 fps to record each subject during each trial. Non-amputee sprinters ran the last 20 m of the straight running trials faster (8.05 ± 0.65 m $\cdot$ s^{-1}) compared to the counterclockwise (7.39 ± 0.49 m $\cdot$ s^{-1}) and clockwise (7.25 ± 0.45 m $\cdot$ s^{-1}) curves ($p=0.002$ and $p=0.001$ respectively). All of the sprinters with leg amputations ran faster during the straight trials (7.82 ± 0.63 m $\cdot$ s^{-1}), compared to curve running with their affected leg on the outside (7.43 ± 0.56 m $\cdot$ s^{-1}) and curve running with their affected leg on the inside (7.05 ± 0.51 m $\cdot$ s^{-1}) ($p=0.001$ for both comparisons). For sprinters with leg amputations, we found that during curve running with the affected leg on the outside the velocities were 4.9% higher, on average, compared to curve running with the affected leg on the inside. This confirms our second hypothesis: the maximum running velocity on curves is limited by the affected leg.

INDEX

1. Introduction

Walking and running are the two basic forms of adult human locomotion. Both gaits involve the repositioning of one leg in front of the other, while pushing with each foot on the ground to support the body and to propel it in the desired direction. Walking and running are usually distinguished by the fact that in walking at least one foot is always touching the ground, while in running there is an "aerial phase" in which no part of the body touches the ground.

Walking is possible only at relatively low speeds: even if we look at competitive walking, maximum speeds are well under 5 $m \cdot s^{-1}$. Above that speed (for non-athletes this limit is around 2.5 $m \cdot s^{-1}$) walking becomes impossible and a running gait is adopted.

Conversely, running is possible from 0 $m \cdot s^{-1}$ (running in place) up to 12 $m \cdot s^{-1}$ (for top level sprinters). Slow speeds can be maintained for a prolonged period of time, while maximum or near-maximum speed can be sustained for just a few seconds. Although low-speed and high-speed are both classified under the definition of "running", there are fundamental differences between them in terms of physiology and biomechanics. Long-distance runners and sprinters have specific body characteristics and compete in separate races, therefore the scientific and technological approach to the study of endurance and sprint running must be tailored to the specific aspects under investigation.

The first measurements on running humans date back since the end of 19th century (see for example figure 1.1).

However, most of the studies were focused on ordinary/average subjects. To better understand how body characteristics influence the biomechanics and the energetics of running, extraordinary subjects and athletes need to be involved. The ability of the human body to adapt and, thanks also to the technological

progresses, to overcome limitations, will help us to better understand the physiology of our “wonderful machine”.

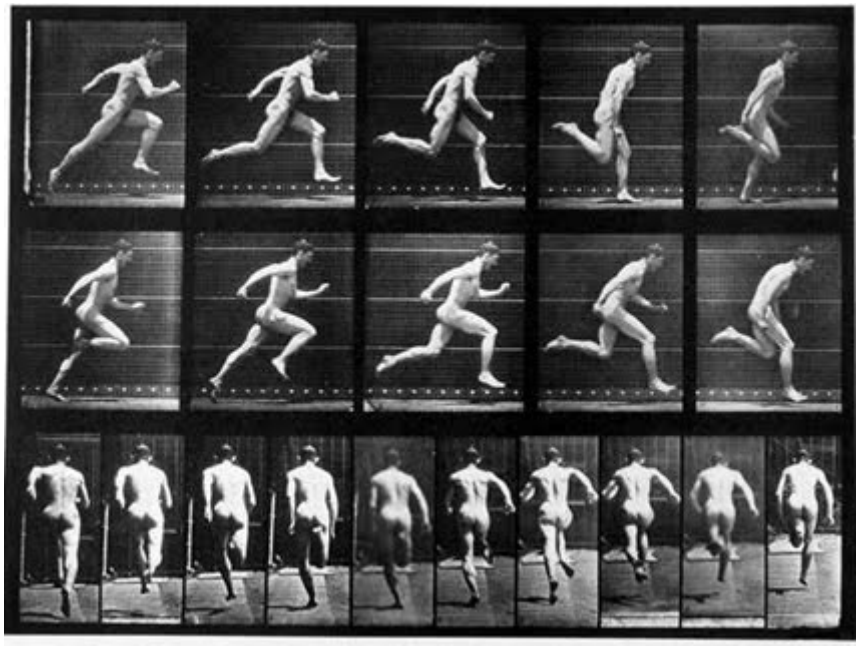

Figure 1.1 - Eadweard Muybridge (1830-1904), "The Human Figure in Motion", 1901

This first chapter of this thesis comprises a brief introduction with some general definitions of the parameters explored throughout the research. Chapter 2 presents the aims of the thesis in greater detail. Chapter 3 describes a study of the influence of body mass on the energetics and mechanics of running, with special emphasis on runners who are obese. Chapters 4 and 5 address the biomechanics of extraordinary athletes who have undergone unilateral leg amputations and now run with running specific prostheses.

1.1 Physiology of muscle contraction

Muscle is a contractile tissue and it's capable of transforming chemical energy into mechanical work. Muscle cells are composed of myofibrils that contain sarcomeres. Sarcomeres can be thought as the basic units of muscle cells and are composed of long, fibrous proteins that slide past each other when the muscles contract and relax. These two proteins are called actin, a thin filament, and myosin, a thick filament with a long, fibrous tail and a globular head which binds to actin (see figure 1.2).

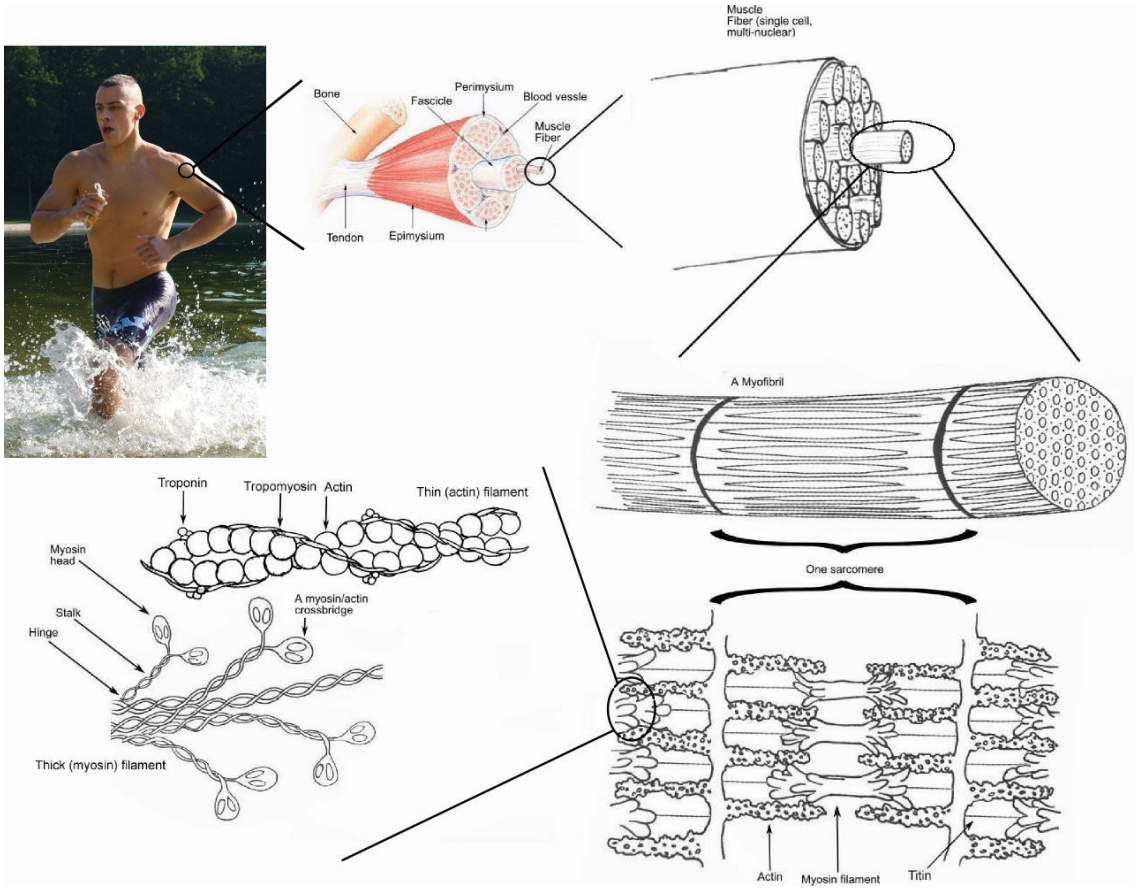

Figure 1.2 - Muscle structure. The sarcomere is the functional unit and muscle contraction is the result of actin-myosin interaction. (http://en.wikipedia.org/wiki/File:Skeletal_muscle.jpg)

Muscle contraction is the result of actin-myosin interaction, driven by ATP hydrolization. Each myosin head bends and pulls the nearby actin fiber, resulting

in an overall shortening of the sarcomere. ATP concentration in resting muscle is limited (~ 5 µmol · g^{-1}) and it allows only a limited number of contractions (Cerretelli, 2001). During muscle contraction under anaerobic conditions, the main energy sources are phosphocreatine (PC,) and glycogen. PC and glycogen substrates allow high intensity muscle contractions for about 6 and 40 seconds respectively, then further activity can be sustained only thanks to oxidative phosphorylation, with a lower power production than the previous mechanisms (figure 1.3).

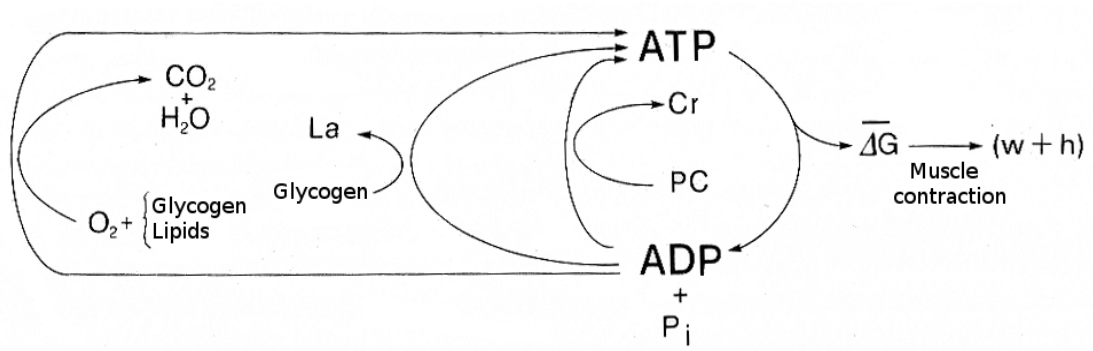

Figure 1.3 - Energy sources of muscle contraction. La, lactate; PC, phosphocreatine; Cr, creatinine. ATP hydrolization releases energy, which is converted into muscle contraction and, as a by-product, heat. ADP is then re-converted to ATP by means the represented processes. (Adapted from di Prampero, 1985)

Energy sources for muscle contraction can therefore be divided into three groups of substances: 1) substances directly used for muscle contraction; 2) substances that can be used only indirectly, through substances of group 1; 3) substances that can be used only indirectly, but depend on oxygen. The advantage of this classification is that maximum available power decreases from group 1 to group 3, while maximum available energy (i.e. the total amount of work capacity) increases from group 1 to group 3.

1.2 Energy sources and exercise intensity

The vast majority of human actions like walking/running at sub-maximal speeds and everyday working activities have relatively low power demands and therefore muscles rely mostly on energy sources belonging to group 3, in particular glycogen and lipids. These two substances are combined with oxygen, providing the necessary energy to re-convert ADP to ATP into the contracting muscles. The chemical reactions of oxygen with glycogen and lipids are well known and the process of calculating the energy production for a given amount of the involved substances is called "indirect calorimetry".

Oxygen consumption ($\dot{V}O_2$, conventionally expressed in $l \cdot min^{-1}$), therefore, provides a measure of the metabolic power demands P (measured in $J \cdot s^{-1}$) of the subject. The total amount of metabolized O_2, leads of course to the total consumed energy E (J), in other terms:

$$E = \int P \, dt \qquad (1.1)$$

A typical example of $\dot{V}O_2$ as a function of time for a constant-load exercise is reported in Figure 1.4. Before t=0 the subject is resting and the measured oxygen consumption is due to the so called "resting metabolic rate". At t=0 the subject begins a "constant load" exercise: an activity with constant power demands. The $\dot{V}O_2$ increases, but its raising is not instantaneous: for the first couple of minutes, despite the constant power developed by the subject, oxygen consumption rises in an exponential way (with a time constant τ_{on} ranging between 20s and 80s) and it reaches a plateau only after 2-3 minutes. At time t=5 minutes, the subject stops exercising and $\dot{V}O_2$ starts decreasing in an exponential way (with a different time constant, τ_{off} of about 25-30s).

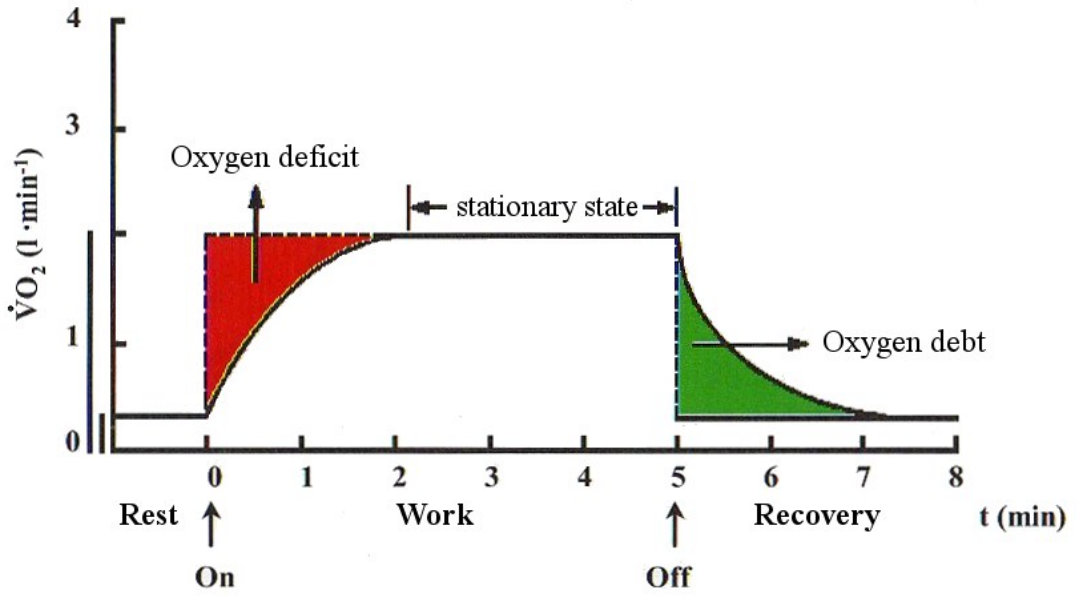

Figure 1.4 - Oxygen consumption ($\dot{V}O_2$, l·min^{-1}) as a function of time during a constant-load exercise. From t=0 to t=2min the subject contracts an "oxygen deficit" which is compensated for during the recovery period by an oxygen uptake exceeding the rest requirements. (Adapted from Cerretelli, 2001)

The measured $\dot{V}O_2$ from minutes 3-5 to the end of the exercise is the so called "stationary state $\dot{V}O_2$" and it varies linearly with work intensity. In these conditions, exercise can be sustained for several minutes and the activities are usually called "aerobic".

Aerobic sources, having only a relatively low power output, can not afford the high-power demands of exercises like sprinting, jumping, weight-lifting and so on. Muscle energy sources rely therefore on the substance belonging to the aforementioned groups 1 and 2. Depending on the required work-load and on the subject's specific training, such high-power activities can be sustained for a couple of minutes or just for 5-6 seconds,. These conditions are called "anaerobic" and are generally divided into two sub-classes: "lactic", when glycogen is utilized, producing lactic acid as a result, and "a-lactic", when only PC is utilized to resynthesize ATP. Lactic anaerobic sources allow a higher power production than aerobic sources, but when lactic acid concentration reaches a certain threshold, the enzymes involved in this mechanism can no longer operate and any further muscle

contraction is stopped. Anaerobic a-lactic energy sources allow even greater power production, but it is limited by PC storages.

At the end of the exercise, O_2 is utilized to resynthesize PC and glycogen storages. However, $\dot{V}O_2$ does not reach a stationary state in this short period of time, therefore oxygen consumption can not be used as a measure of the instantaneous energy demands of a subject performing explosive or sprint exercises.

1.3 Energy cost of locomotion

When studying locomotion, a useful measure of energy expenditure is the *energy cost* of locomotion C^T (also called *cost of transport*), defined as the energy expenditure E divided by the travelled distance d:

$$C^T = E/d \qquad (1.2)$$

C^T is measured in $J \cdot m^{-1}$ and is defined as the *total* energy cost of locomotion, in order to distinguish it from the *mass-specific* energy cost of locomotion C (in $J \cdot m^{-1} \cdot kg^{-1}$) obtained by dividing C^T by the body mass of the subject.

The cost of transport for walking can be described roughly by a quadratic function of speed, having the vertex at the "optimal walking speed" (see figure 1.5). When a subject walks slower or faster than this speed, the cost of transport increases. Optimal walking speed can be predicted by the dimensionless Froude number:

$$Fr = \frac{v^2}{gL} \qquad (1.3)$$

where v is the walking speed (in $m \cdot s^{-1}$), g is the acceleration due to gravity (9.81 $m \cdot s^{-2}$) and L is the leg length (measured in m).

The optimal walking speed is attained at $Fr = 0.25$ (Saibene and Minetti, 2003).

Above a certain point (corresponding to $Fr = 0.5$, about 2 $m \cdot s^{-1}$ for a medium-sized human) running becomes the more economical way to move. The cost of transport of running is independent of speed (di Prampero, 1985), if we discard air-resistance (for example when the subject is running at low speeds or on a treadmill). Air resistance, in contrast, plays a major role in other forms of locomotion, like speed ice-skating and biking, where much higher speeds are reached.

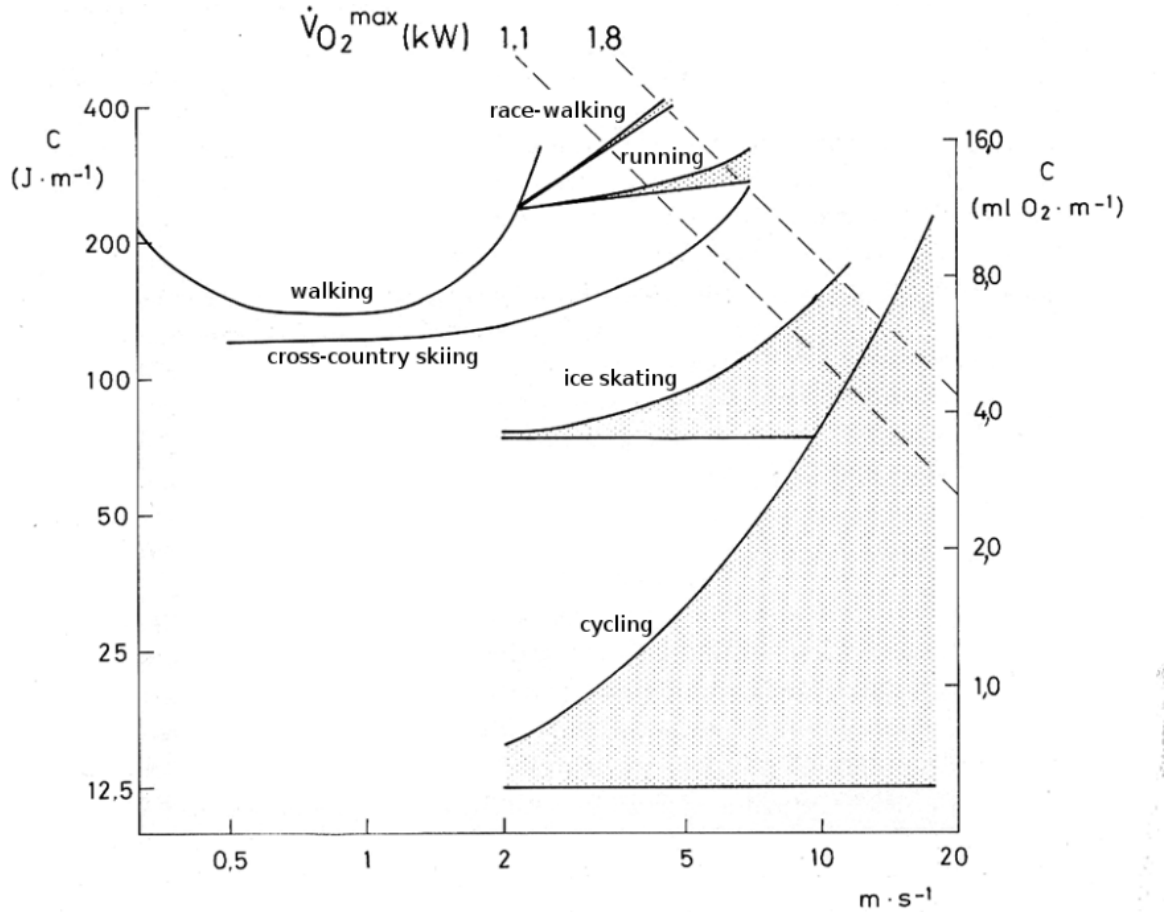

Figure 1.5 - Energy cost of various forms of locomotion as a function of speed, for a subject of 75 kg of mass and 1.75 m of height. Lower lines refer to non-aerodynamic energy cost, the upper lines the total cost. The dashed lines refer to a non-trained subject (1.1 kW) and to an elite-level athlete (1.8 kW). (Adapted from di Prampero, 1985)

1.4 Mechanical aspects of locomotion

When muscle shortens upon contraction, chemical energy is converted into mechanical energy and actual work is performed. Work (W, measured in J) is defined as the vector product:

$$W = \vec{f} \times \vec{d} \qquad (1.4)$$

where $\vec{f}$ is the applied force (measured in N) and $\vec{d}$ is the displacement (measured in m).

The performed work is then converted into elastic energy through the deformation of passive tissues (mainly tendons and ligaments) and finally into kinetic and potential energy, whose respective general definitions are:

$$E_k = \frac{1}{2}mv^2 + \frac{1}{2}I\omega^2 \qquad (1.5)$$

$$E_p = mgh \qquad (1.6)$$

where, for a generic object, m (measured in kg) is the mass, v (measured in $\mathrm{m \cdot s^{-1}}$) is the velocity, I (measured in $\mathrm{kg \cdot m^2}$) is the moment of inertia, ω (measured in $\mathrm{rad \cdot s^{-1}}$) is the angular velocity and h (measured in m) is the altitude.

Therefore, the total mechanical energy of the human body, divided into n rigid segments, is:

$$E_{tot} = \sum_{i=1}^{n} E_{k\,i} + E_{p\,i} \qquad (1.7)$$

where $E_{k\,i}$ and $E_{p\,i}$ are the kinetic and potential energy of the ith segment (figure 1.6).

Since the linear velocity v_i of the ith body segment can be expressed as:

$$v_i = v_{CoM} + v_{r,i} \qquad (1.8)$$

where v_{CoM} is the velocity of the *Center of Mass* (CoM) relative to the surroundings and $v_{r,i}$ is the velocity of the ith segment relative to the CoM, equation 1.7 can be rewritten as:

$$E_{tot} = MgH_{CoM} + \frac{1}{2}Mv_{CoM}^2 + \sum_{i=1}^{n}\left(\frac{1}{2}m_i v_{r,i}^2 + \frac{1}{2}I\omega_i^2\right) \quad (1.9)$$

where M is the mass of the whole body and H_{CoM} the altitude of the CoM (Willems et al. 1995).

1.4.1 Mechanical work during constant speed running

When a subject is running at constant speed on flat terrain, the total mechanical energy E_{tot} has an oscillating pattern with the same period T of the gait cycle, as reported in figure 1.6. In other terms:

$$E_{tot}(t+T) = E_{tot}(t) \quad (1.10)$$

From a "purely mechanical" point of view, therefore, the subject is not performing any work:

$$W = \Delta E_{tot} = 0 \quad (1.11)$$

However, human tissues are not ideal machines: when the subject touches the ground, only a part of E_{tot} is absorbed by tendons and other elastic tissues in order to be released at the subsequent part of the step. In addition, when muscles perform negative work (eccentric contraction: vectors $\vec{F}$ and $\vec{d}$ have opposite directions in equation 1.4) or no work at all (isometric contraction: $\vec{d} = 0$ in equation 1.4) they still consume a positive amount of energy.

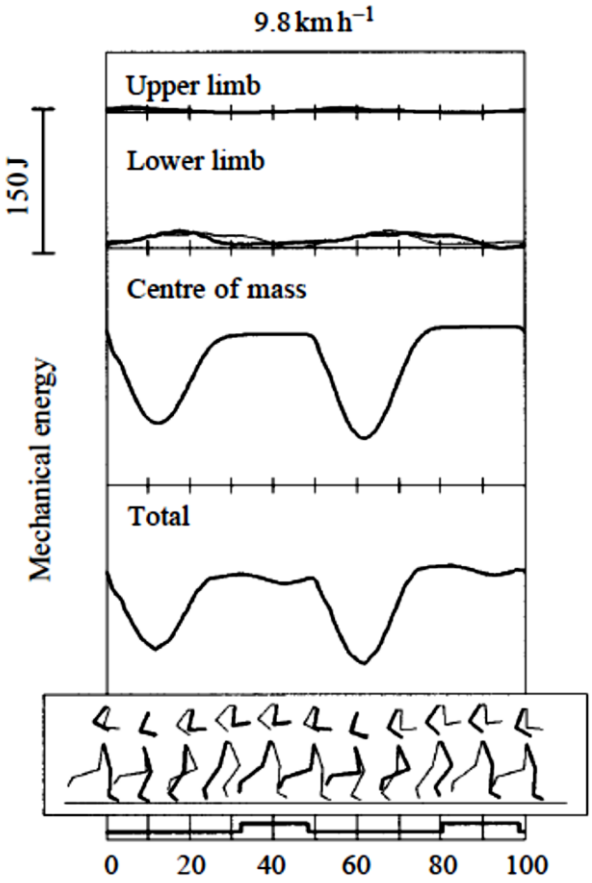

Figure 1.6 - Mechanical energy of a subject running at 9.8 km·h^{-1}. The two upper panels indicate the Ek changes of the upper and lower limbs, due to their movement relative to the CoM, calculated by adding the Ek curves of the segments of each limb. The third panel indicates the mechanical energy of the CoM ($MgH + 1/2Mv_{CoM}^2$). The fourth panel indicates the E_{tot} of the body, calculated by summing the curves in the three upper panels; the sum of the increments in this curve represents the W_{tot} (Willems et al. 1995).

The exact contribution of elastic tissues, and therefore of negative work done by muscles, is problematic and a convenient approach is to discard negative variations of E_{tot} in the calculation of the performed mechanical work (Cavagna et al. 1977).

The sum of the *positive increments* of the first two terms on the right side of equation 1.9 ($MgH + 1/2Mv_{CoM}^2$) is called the total external work W_{ext}^Twhile the sum of the *positive increments* of the other terms ($\sum_{i=1}^{n}(1/2m_i v_{r,i}^2 + 1/2I\omega_i^2)$) is called the total internal work W_{int}^T.

External work can be thought as the mechanical work performed by the muscles to lift and accelerate the whole body, while internal work as the mechanical work performed to rotate and accelerate the limbs relatively to the CoM.

The sum of total external and total internal work leads to total mechanical work:

$$W_{tot}^{T} = W_{ext}^{T} + W_{int}^{T} \qquad (1.12)$$

Also W_{tot}^{T}, W_{ext}^{T} and W_{int}^{T}, are usually divided by the travelled distance and therefore are expressed in J · m^{-1}. *Mass-specific* total, external and internal works (W_{tot}, W_{ext} and W_{int} respectively, measured in J · m^{-1} · kg^{-1}) are then obtained by dividing each value by the mass of the subject.

The product of mass-specific mechanical work and locomotion speed leads to mass-specific mechanical power:

$$P_M = W_{tot} \cdot v \qquad (1.13)$$

measured in J · s^{-1} · kg^{-1} (or W · kg^{-1}).

1.4.2 Mechanical work during accelerated running

During the acceleration phase of sprint running, a subject increases v_{CoM}; in addition, if the sprinter uses a crouched starting position, he/she also increases H_{CoM}. The total mechanical energy at the end of a complete stride cycle of duration T is therefore increased:

$$E_{tot}(t+T) > E_{tot}(t) \qquad (1.14)$$

and the actual performed work is:

$$W = \Delta E_{tot} > 0 \qquad (1.15)$$

From equations 1.4 and 1.15, it necessary follows that the mean resultant force is:

$$\vec{f} = \overrightarrow{GRF} + \overrightarrow{BW} > 0 \qquad (1.16)$$

where the + sing indicates the vector sum of $\overrightarrow{GRF}$, the ground reaction force, and $\overrightarrow{BW}$, the body weight. $\vec{f}$ can be projected in the horizontal and vertical directions:

$$\vec{f} = \vec{f}_x + \vec{f}_z \qquad (1.17)$$

where, again, the + sign indicates the vector sum of the horizontal ($\vec{f}_x$) and vertical ($\vec{f}_z$) force components.

The performed work in the horizontal and vertical direction can be calculated as:

$$W_x^T = \int f_x dx \qquad (1.18)$$

$$W_z^T = \int f_z dz \qquad (1.19)$$

where dx and dz are the infinitesimal displacements along horizontal and vertical directions respectively. Of course f_x and f_z vary with time, therefore the performed work is not constant in accelerated running, unlike constant speed running.

The total performed work can be calculated as the sum of the horizontal and vertical contributions:

$$W_{tot}^T = W_x^T + W_z^T \qquad (1.20)$$

W_{tot}^T, W_x^T and W_z^T, can be divided by the travelled distance and therefore are expressed in $J \cdot m^{-1}$. *Mass-specific* total, horizontal and vertical works (W_{tot}, W_x and W_z respectively, measured in $J \cdot m^{-1} \cdot kg^{-1}$) are then obtained by dividing each value by the mass of the subject.

Mass-specific mechanical power, measured in $W \cdot kg^{-1}$, can be divided in the horizontal and vertical directions:

$$P_x = {}^{dW_x}/_{dT} = f_x \, {}^{dx}/_{dt} = f_x v_x \qquad (1.21)$$

$$P_z = {}^{dW_z}/_{dT} = f_z \, {}^{dz}/_{dt} = f_z v_z \qquad (1.22)$$

where v_x and v_z are the horizontal and vertical vector components of v_{CoM}. The total mass-specific power is:

$$P_{tot} = P_x + P_z \qquad (1.23)$$

as f_x, f_z, v_x and v_z vary with time, also P_x and P_z vary with time.

1.4.3 Efficiency

The ratio between performed work W and energy expenditure E yields the efficiency:

$$\eta = W/E \cdot 100 \qquad (1.24)$$

where W and E must be expressed in the same units (J, J · m^{-1} or J · m^{-1} · kg^{-1}), therefore efficiency is a dimensionless measure, expressed in percentage (Cavagna and Kaneko 1977).

1.4.4 Applied forces during straight and curve running

When a subject is moving at constant speed on a straight path, his/her average acceleration is zero; therefore the average resultant force, calculated over an entire step (i.e. from foot contact to contralateral foot contact), is zero. Equation 1.16 becomes:

$$\vec{f} = \overrightarrow{GRF} + \overrightarrow{BW} = 0 \qquad (1.25)$$

This means that the average magnitude of the vertical ground reaction force equals the magnitude of body weight:

$$\overline{GRF_v} = BW \qquad (1.26)$$

During running there is a period when both limbs are off the ground, called the "aerial time". This implies that during foot contact GRF_v must exceed BW (see figure 1.7). During sprinting, foot contact time decreases and aerial time remains almost unchanged, consequently GRF_v can reach magnitudes of more than 2 BW (Weyand et al. 2000).

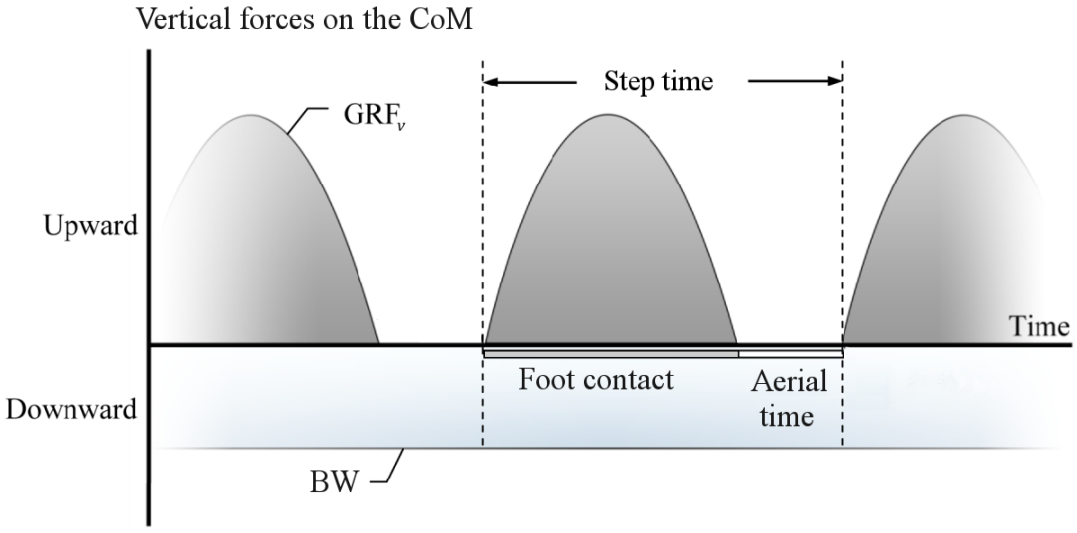

Figure 1.7 – Vertical forces acting on a subject running on a straight path at constant speed. Body weight is directed downwards and is constant, ground reaction force (GRF_v) is directed upwards and is applied only during foot contact. (Adapted from Luo, 2012)

During curve running, the CoM of the subject is accelerating towards the instant center of rotation with a magnitude:

$$a_c = {v_{CoM}^2}/{r} \qquad (1.27)$$

where v_{CoM} is the velocity of the CoM, r is the radius of the curve and a_c is the centripetal acceleration. To obtain a_c, the subject must apply a centripetal ground reaction force (GRF_c) with the following average magnitude:

$$\overline{GRF_c} = F_c = M \cdot {v_{CoM}^2}/{r} \qquad (1.28)$$

where F_c is the centripetal force and M is the mass of the subject. Given that GRF_c can act on the subject's CoM only during foot contact, the value of GRF_c during foot contact must exceed F_c.

The total ground reaction force during curve running is:

$$\overrightarrow{GRF} = \overrightarrow{GRF_v} + \overrightarrow{GRF_c} \qquad (1.29)$$

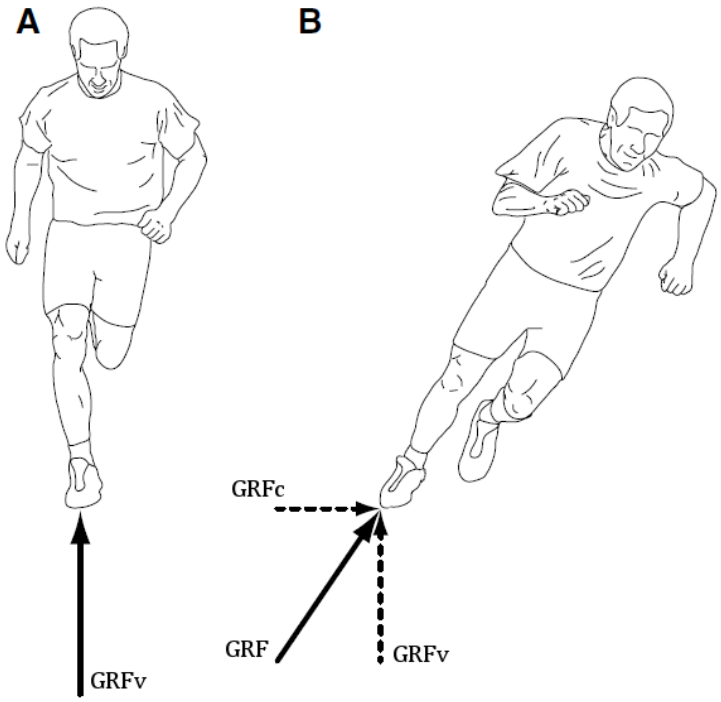

Figure 1.8 Ground reaction forces (GRF) on a sprinter along a straight path (A) and on a curved path (B). (Adapted from Chang and Kram, 2007)

1.5 References

Cavagna GA, Heglund NC, Taylor CR. (1977). Mechanical work in terrestrial locomotion: two basic mechanisms for minimizing energy expenditure. American Journal of Physiology-Regulatory, *Integrative and Comparative Physiology*, 233(5), R243-R261.

Cavagna GA, Kaneko M. (1977). Mechanical work and efficiency in level walking and running. *The Journal of physiology*, *268*(2), 467-481.

Cerretelli P. (2001). Fisiologia dell'esercizio: sport, ambiente, età, sesso. SEU.

di Prampero PE. (1985). La locomozione umana su terra, in acqua, in aria: fatti e teorie. Ediermes.

Luo, G. (2012). *Limiting Factors for Curved Sprinting Performance* (Doctoral dissertation, University of Calgary).

Saibene F, Minetti AE. (2003) Biomechanical and physiological aspects of legged locomotion in humans. *Eur J Appl Physiol* 88: 297–316

Willems PA, Cavagna GA, Heglund NC. (1995). External, internal and total work in human locomotion. *Journal of Experimental Biology*, 198(2), 379-393.

Weyand, P., Sternlight, D., Bellizzi, M., and Wright, S. (2000). Faster top running speeds are achieved with greater ground forces not more rapid leg movements. *Journal of Applied Physiology*, 89, 1991-9

2. Aims of the thesis

This thesis is divided in two main parts, which reflect the two research topics explored during my Ph.D. program:

Part I: the effect of body mass on the energetics and biomechanics of running. The aim of this study was to investigate the mechanical work, energy cost of transport, and efficiency during running in normal-weight and obese men.

Part IIa: optimal starting block configuration in sprint running; a comparison of biological and prosthetic legs. The aim of this study was to measure the effect of starting block configuration on starting performance of both non-amputee sprinters and athletes with unilateral transtibial amputations.

Part IIb: maximum speed curve running of sprinters with and without unilateral leg amputations. The aim of this study was to compare curve running performance between non-amputee sprinters and sprinters with unilateral transtibial amputations.

3. Part I: Energetics and mechanics of running men, the influence of body mass

3.1 Introduction

The Froude number described in chapter 1.3 (see equation 1.3), although developed by naval engineer William Froude for the study of the behavior of real ships from smaller models, fairly belongs also to a particular branch of biology called allometry. Firstly outlined by Otto Snell in 1892 and Julian Huxley in 1932, allometry is the study of the relationship of shape, anatomy, physiology, and finally behavior to body size of animals of different types in terms of size/mass and also species.

In fact, Alexander (1984) showed that animals of different sizes, running with equal Froude numbers, tend to dynamic similarity: they use the same gait, similar relative stride lengths and duty factors, and exert similar patterns of force on the ground.

Froude number is not the only measure than can be applied in allometry, in general a typical allometric equation, called also the equation of simple allometry (Alexander, 1982), has the following form:

$$y = ax^b \qquad (3.1)$$

where x and y are the investigated dimension or properties in animals of different sizes and the factor a and exponent b are constants. By taking logarithms, equation 3.1 can be changed into:

$$\log y = \log a + b \log x \qquad (3.2)$$

$$Y = A + bX \qquad (3.3)$$

in order to calculate regression coefficients and confidence intervals. Usually the constant b is most informative and is called the primary allometric signal (Kram, 2012).

A series of four papers by Heglund, Taylor et al. (Fedak et al. 1982; Heglund et al. 1982a, b; Taylor et al. 1982) investigated in particular the link between energetics and mechanics as a function of body size in birds and mammals. The major part of their work was carried out in Kenya and included a number of wild and domestic animals. The wild artiodactyls had a mass ranging from 3.5 kg (suni: a small antelope, *Nesotragus moschatus*) to 213 kg (eland: a big sized antelope, *Taurotragus oryx*). The domestic artiodactyls had a mass ranging from 20 kg (african goat: *Capra hircus*) to 254 kg (zebu cattle: *Bos indicus*). They also measured three species of small carnivores (dwarf mongoose, *Helogale pervula*; anded mongoose, *Mungos mungo*; genet cat, *Genetta tigrina*) with masses ranging from 0.583 kg to 1.46 kg. In addition, in the United States they were also able to measure primates (from the 0.124 kg of the tree shrew, *Tupaia glis*, to the 8.50 kg of hamadryas baboon, *Papio hamadryas*), rodents (flying squirrel, *Glaucomys volans*, with an average body mass of 0.063 kg) and carnivores (from the 0.542 kg of the ferret, *Mustela nigripes*, to 23.1 kg of the wolf, *Canis lupus*).

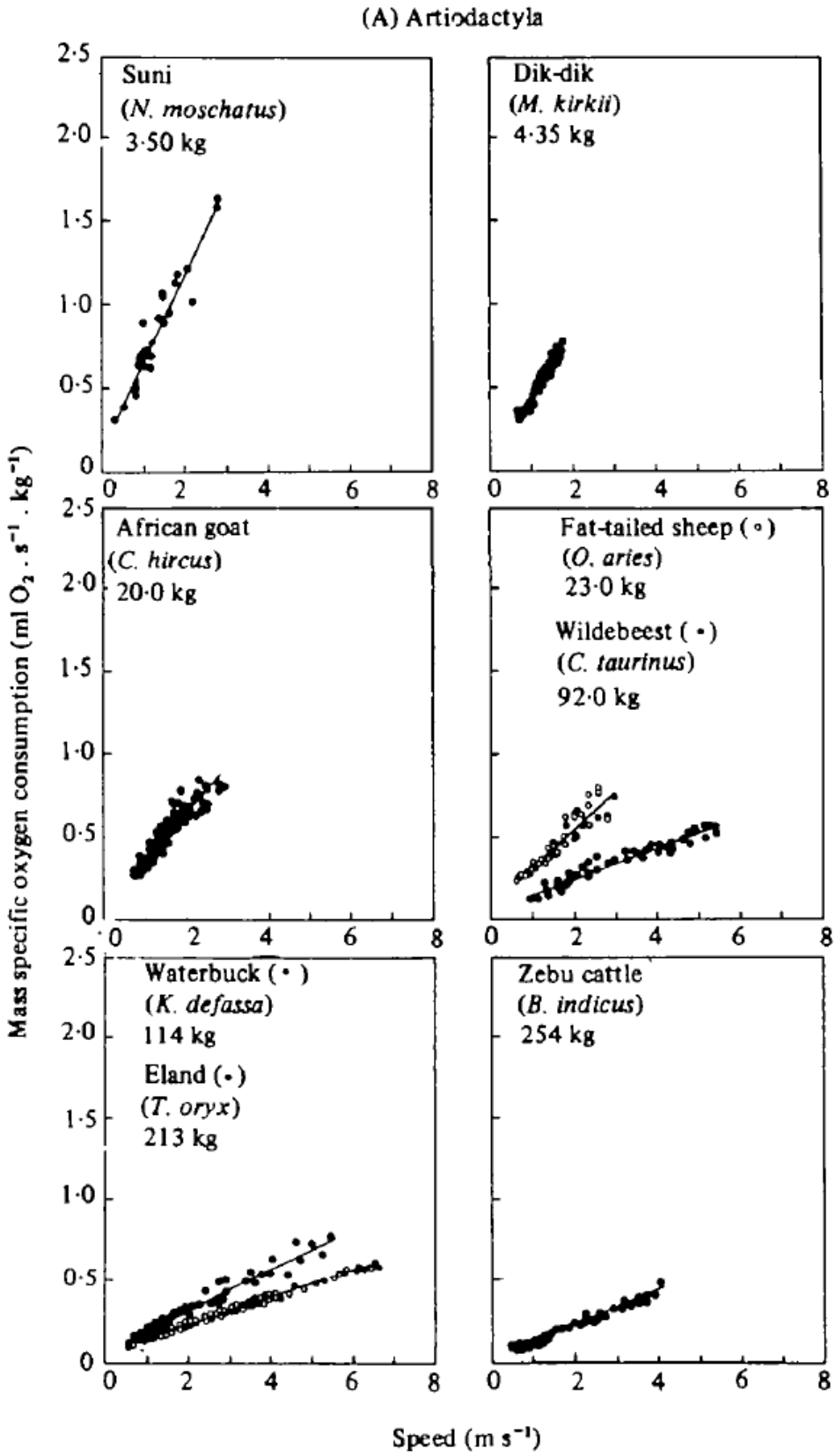

Figure 3.1 - Mass-specific oxygen consumption, $\dot{V}O_2/M$ ($mlO_2 \cdot s^{-1} \cdot kg^{-1}$) plotted as a function of speed (m·s-1) for artiodactyls. Similar graphs were obtained for carnivores, primates and rodents (Taylor et al. 1982).

As reported in figure 3.1 the relationship between mass-specific oxygen consumption and speed for each animal can be expressed as:

$$\dot{V}O_2/_M = slope \cdot speed + Yintercept \qquad (3.4)$$

$Yintercept$ in equation 3.4 represents the metabolic rate while standing still, while the $slope$ is the mass-specific energy cost C. Combining mass-specific energy cost of all 20 species with literature data for 42 other species of birds and mammals, Taylor et al. found the following allometric law:

$$C = 10.71 \cdot M^{-0.316} \qquad (3.5)$$

(in the original paper, C was measured in $mlO_2 \cdot m^{-1} \cdot kg^{-1}$, here we converted it into in $J \cdot m^{-1} \cdot kg^{-1}$).

In other terms, equation 3.5 states that, as the overall mass of an animal increases, C decreases: a mouse uses approximately 40 times more energy than an elephant to carry 1g of its mass over the same distance (Langman et al. 1994).

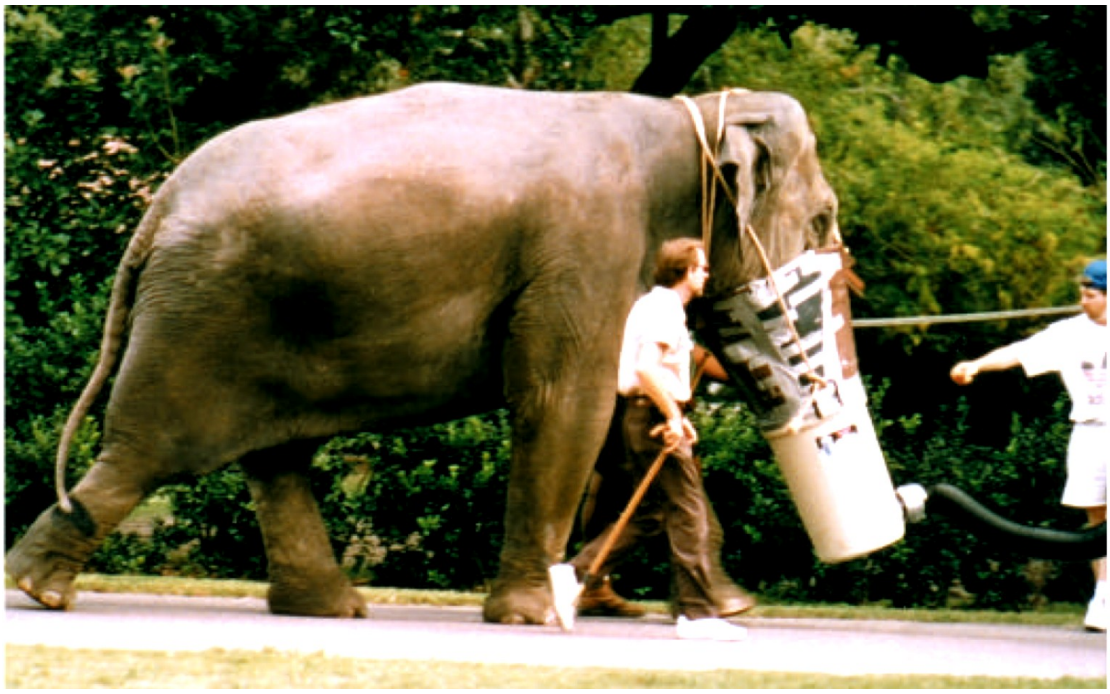

Figure 3.2 - An African elephant wearing a mask for $\dot{V}O_2$ measurements (Langman et al. 1994).

Heglund, Taylor et al. observed that the mass-specific mechanical power (see equation 1.11) in a number of animal species increases with the speed as described by:

$$P_M = 0.478 \cdot v^{1.53} + 0.685 \cdot v + 0.072 \qquad (3.6)$$

P_M in equation 3.6 is independent of the overall mass of the animal. It also follows that, at variance with the mass-specific cost of transport (equation 3.5), the mass-specific mechanical work, as obtained from the ratio of equation 3.6 to speed, is independent of the animal's body mass, as described by:

$$W_{tot} = 0.478 \cdot v^{0.53} + 0.685 + 0.072 \cdot v^{-1} \qquad (3.7)$$

see also figure 3.3.

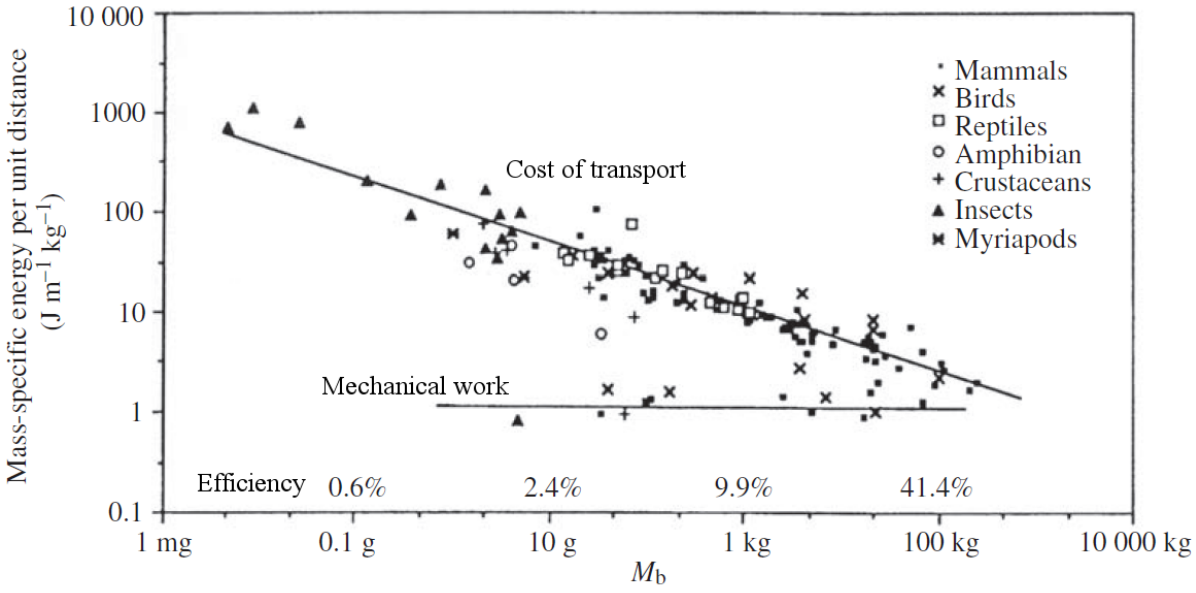

Figure 3.3 – Energy cost C, mechanical work W_{tot} and efficiency η (as a function of body mass of different animals). C is independent of speed, while $W_{tot}$and η are calculated for v = 1 m·s^{-1} (adapted from Alexander, 2005)

The ratio of equations 3.7 and 3.5 (multiplied by 100) yields the efficiency:

$$\eta = (4.46 \cdot v^{0.53} + 6.40 + 0.67 \cdot v^{-1}) \cdot M^{0.316} \quad (3.8)$$

For each given speed, animals of increasing sizes have increasing efficiency: a 0.01 kg mouse (*Mus musculus*) moving at 1 $m \cdot s^{-1}$, for example, has an efficiency of about 2.7 %, while a 1500 kg african elephant (*Loxodonta africana*) has a 100% efficiency. Efficiency values greater than ~25% (Hill, 1922) can be explained by the fact that during locomotion a large fraction of mechanical energy is stored and released by the elastic tissues of the limbs (mainly tendons and ligaments), allowing lower metabolic energy demands. Equation 3.8 shows that this contribution increases as the overall mass of the animal grows and with increasing speed (see figures 3.3 and 3.4 respectively).

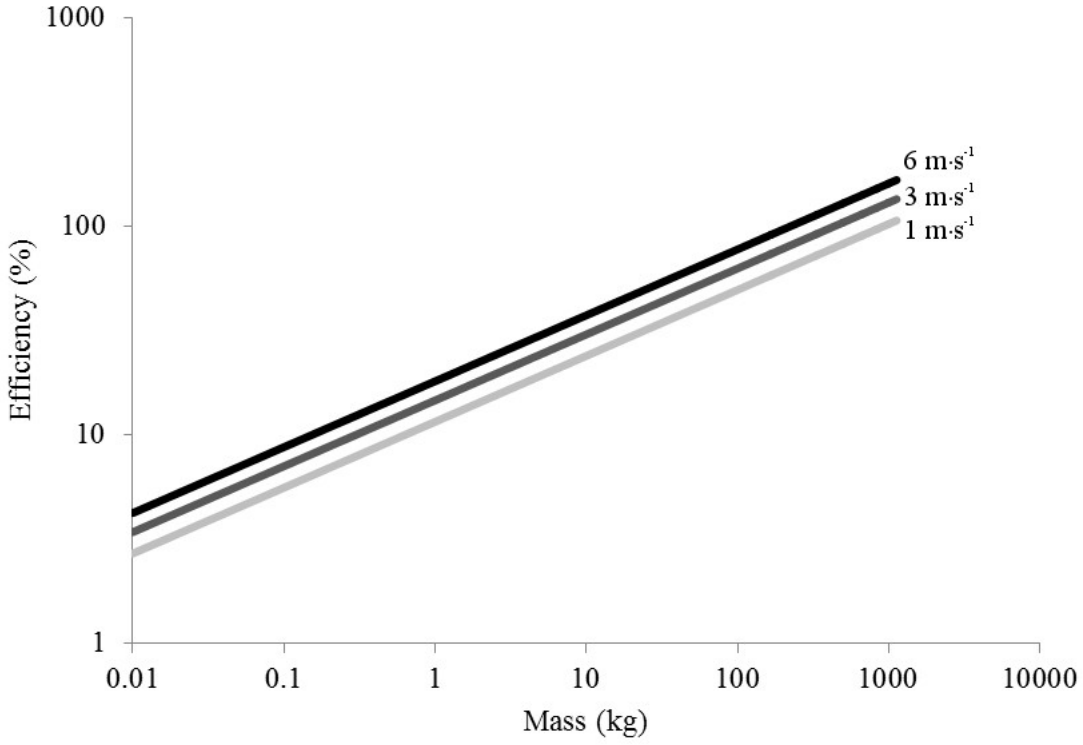

Figure 3.4. Efficiency as a function of body mass of different animals moving at 1, 3 and 6 $m \cdot s^{-1}$ of speed. Efficiency increases with mass and with speed of locomotion.

3.2 Aims of the study

The knowledge of the relations between physiological and mechanical cost of transport and body dimensions in humans is rather scanty. Considering that humans differ widely in body dimensions, our initial hypothesis was that the relationship between mechanical and energy cost of transport and body mass in running followed the allometric laws described by Heglund, Taylor et al. (1982). Therefore, the purpose of this study was to investigate mechanical work, energy cost of transport and efficiency during running in normal-weighted and obese subjects.

3.3 Research design and methods

3.3.1 Subjects

Ten severely obese and 15 normal-weighted boys and men, aged 16-40 years, participated in this study. We recruited the obese subjects among hospitalized patients at the Divisions of Auxology (adolescents) and Metabolic Diseases (adults), Italian Institute for Auxology, Piancavallo (VB), Italy, while the normal-weighted subjects were recruited and tested in the Laboratories of the Sport Sciences School, University of Udine, Udine, Italy.

All obese adolescents had body mass index (BMI) values higher than +2 SD from the means for age and sex, evaluated using the national BMI charts (Cacciari et al. 2006) and all obese adults had BMI values above 35 $kg \cdot m^{-2}$, whereas the BMI values of all the normal-weighted adolescents were comprised between -1 SD and +1 SD of the mean values for the age and sex (Cacciari et al. 2006) and those of normal-weighted adults had BMI values between 20 and 25 $kg \cdot m^{-2}$. Obese and normal-weighted subjects who had previously participated in weight management programs, or had overt metabolic and/or endocrine diseases, and those taking medications regularly or using any drugs known to influence energy metabolism were excluded. Previous studies showed a correlation between energy cost of transport and stature (Bourdin et al. 1993); normalweighted subjects whose stature was outside ±2 SD from the mean value of the obese group were therefore excluded.

The study was conducted in accordance with the Declaration of Helsinki and the experimental protocol was approved by the Ethics Committee of the Italian Institute for Auxology (Milan). Before the study began, the purpose and objectives were carefully explained to each subject and written informed consent was obtained from all subjects or from their parents for minors.

3.3.2 Physical characteristics and body composition

Body mass (**M**) was measured to the nearest 0.1 kg with a manual-weighing scale (Seca 709, Hamburg, Germany) with the subject dressed only in light underwear and no shoes. Stature was measured to the nearest 0.5 cm on a standardized wall-mounted height board. Body mass index (BMI) was calculated as **M** (kg) $\times$stature^{-2} (m).

Body composition was assessed by bioelectric impedance analysis (BIA) performed in accordance with the conventional standard technique (Lukaski et al. 1986). This method involves the placement of 2 couples of electrodes on the ipsilateral wrist and ankle of the supine subjects (see figure 3.5a), an current A (50 kHz, 0.8 mA) is applied through the first couple of electrodes (I_1, I_2), while the second couple (E_1, E_2) is used to measure the voltage drop V (see Figure 3.5b). Subject's electrical impedance ($Z_{subject}$) in calculated as the ratio between V and A.

Fat free mass (FFM) tissue impedance is much lower than that of fat mass (FM), therefore by measuring $Z_{subject}$ it is possible to calculate the FM percentage of a given subject. These measurements were made with Human-IM system (Dietosystem, Italy), FFM and FM were obtained from the software provided by the manufacturer.

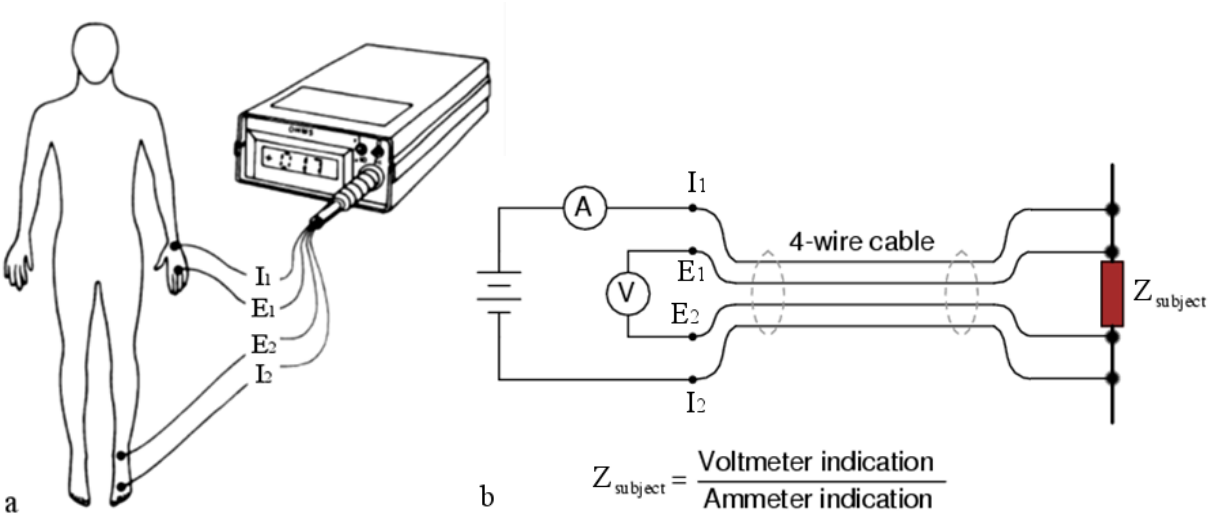

Figure 3.5 - Bioelectric impedance analysis (BIA): electrodes placement on the subject (a) (adapted from Lukaski et a. 1985), circuit diagram (b) (adapted from www.allaboutcircuits.com).

3.3.3 Experimental design

Energy cost of running was measured during an exercise test on a treadmill (Saturn, HP Cosmos, Germany) under medical supervision. After 8 min of rest in the standing position on the treadmill, the subject ran at 2.2 $m \cdot s^{-1}$ (8 $km \cdot h^{-1}$). During this period $\dot{V}O_2$ was determined as described below and the subjects were filmed with four cameras (described below) for kinematic analysis. Before the actual experimental sessions, the subjects were familiarized whit the laboratory procedures by having them run in three different days for at least 10 min at 1.9, 2.2 and 2.5 $m \cdot s^{-1}$ (7, 8, and 9 $km \cdot h^{-1}$) while wearing nose clip and respiratory valve (described below). During these tests we observed that some subjects walked at 1.9 $m \cdot s^{-1}$; however, all of them ran at 2.2 and 2.5 $m \cdot s^{-1}$. A running gait was acknowledged when, in contrast to walking, an aerial phase was clearly visible and the subject had no double-support phase. In addition, two different samples of expired air were collected between minutes 6 and 8, and minutes 8 and 10 at all speeds. Only at 2.2 $m \cdot s^{-1}$ no differences in $\dot{V}O_2$, rate of carbon dioxide production

($\dot{V}CO_2$), expiratory exchange ratio (RER) and C were observed between these two periods and between groups, which indicate that a "true" steady-state was reached.

Three familiarization sessions were considered sufficient in view of the results reported by Brueckner et al. (1991), even if we are not aware of any similar study on obese subjects.

3.3.4 Energy cost of running

To measure $\dot{V}O_2$ during rest and running, we used the classical Douglas bag method: the expired gases were collected in aluminized bags (Series 600, Hans Rudolph Inc., Kansas City, MO) that have extremely low gas permeability.

Expired gas was collected both at rest and exercise while the subjects, wearing a nose clip, breathed through a low-resistance Hans Rudolph R2700 respiratory valve (131 g) (Kansas City, MO). A 2 m length of corrugated tubing (internal diameter = 3.8 cm) connected the expiratory port of the respiratory valve to the Douglas bags.

The gas fractions in the expired gas collected at steady-state for a timed period were analyzed by a O_2 and CO_2 analyzer (5200 Multi Purpose, Servomex Group Ltd., UK) previously calibrated by means of a known gas mixture (16 % O_2, 4 % CO_2 in N_2). Expired gas volume was measured by means of a calibrated dry gas meter (Model 516163, Harvard Apparatus Ltd., UK) and corrected for the 600 ml extracted by the O_2 and CO_2 analyzer. The tests were performed in the morning under medical supervision and consisted of an 8-min rest period (standing on the treadmill) followed by an 8-min run on the level at 2.2 $m \cdot s^{-1}$ (Margaria et al. 1963; di Prampero 1986) with continuous 12-lead ECG monitoring. The resting metabolic rate was determined during the last 3 min of rest, whereas the exercise steady-state $\dot{V}O_2$ was determined from min 6 thorough 8 of the running period.

The oxygen cost of running ($mlO_2 \cdot min^{-1}$) was calculated by dividing the steady-state oxygen uptake ($\dot{V}O_2$), above the value measured at rest in standing position, by the running speed. The so obtained values were converted into total energy cost of running C^T ($J \cdot m^{-1}$) on the basis of an O_2 energy equivalent estimated from individual RER values, assumed to be equal to the metabolic respiratory quotient (RQ).

Mass-specific energy cost of running C ($J \cdot m^{-1} \cdot kg^{-1}$) was calculated dividing the total energy cost of running C^T by the mass of the subject.

3.3.5 External mechanical work

The position of CoM was calculated via three-dimensional stereophotogrammetry. Four video-cameras (Canon XM2, 720 9 576 pixel, 50 $fields \cdot s^{-1}$) were placed around the treadmill, a parallelepiped aluminum frame (1x1x2m) was used to reconstruct the position of each video-camera by means of a direct-linear-transform (DLT) algorithm implemented into Simi Motion 3D software (Simi reality motion systems – Germany). We positioned three reflective markers on the subject's body: over the right and left spina iliaca superior and over the second lumbar vertebra. Simi Motion software was used also to track and reconstruct the three-dimensional position of each marker. As shown by Diss (2001) and Nolan et al. (2006), an acquisition frequency of 50 Hz is amply sufficient to assess kinematic variables during low-speed running.

The tracked data were filtered through a moving-average filter (radius = 1) and the position of CoM was calculated as the mean position of the three markers(Myers and Steudel 1985, Bourdin et al. 1995).

For each subject, 10 subsequent ‘‘representative’’ steps (i.e., without anomalous movements of limbs, torsion of head or trunk, etc.) were analyzed by means of a custom-made Matlab program. The program performed the same calculations showed in chapter 1.3 to obtain total and mass specific external work (W_{ext}^T and W_{ext} respectively). All three spatial directions were taken in account for kinetic energy calculations, for the antero-posterior direction (Y axis, see figure 3.6), the treadmill speed was taken in account when calculating the kinetic energy of the CoM. For each subject, efficiency η was calculated according to equation 1.13.

3.3.6 Statistical analyses

Statistical analyses were performed using Statistica for Windows (Kernel version 5.5 A, StatSoft, Maisons-Alfort, France) with significance set at $p<0.05$. All results were expressed as means and standard deviation (SD). The effects of group (obese vs. normal-weighted subjects) on physical and physiological capacities were tested using unpaired Student's t test. Relationships between variables were investigated using Pearson's product-moment correlation coefficient.

3.4 Results

3.4.1 Physical characteristics of subjects

The physical characteristics of obese and normal-weighted subjects are shown in table 3.1. Obese had a significantly higher mean age (+9.2 years, $p = 0.014$) and mean body mass (+66.6 kg, $p < 0.001$) than normal-weighted subjects, as well as greater FFM (+28.3 kg, $p < 0.001$) and %FM (+10.5 %, $p < 0.001$).

	Obese (n=10)			Normal weighted (n=15)			p
Age (years)	27.2 ± 11.2	[16.0 - 45.8]		18.2 ± 7.8	[16.1 - 40.0]		0.014
Body mass (kg)	130.7 ± 23.7	[108.5 - 172]		64.1 ± 10.3	[52.0 - 89.0]		0.001
Stature (m)	1.77 ± 0.07	[1.67 - 1.89]		1.72 ± 0.08	[1.60 - 1.88]		0.124
BMI ($kg \cdot m^{-2}$)	41.5 ± 5.3	[35.8 - 48.6]		21.6 ± 2.4	[20.1 - 24.4]		0.001
FFM (kg)	80.0 ± 13.3	[66.7 - 104.3]		51.7 ± 8.0	[36.8 - 72.1]		0.001
FM (%)	38.6 ± 1.9	[35.5 - 42.2]		19.1 ± 6.0	[11.2 - 30.9]		0.001

Table 3.1 - Physical characteristics of subjects. All values are mean and standard deviation (SD). Minimum and maximum values in brackets. BMI: Body mass index; FFM: Fat-free mass; FM: Fat mass, p: Significance by Student's t-test. All values are mean and standard deviation (SD). Minimum and maximum values in brackets

3.4.2 Total energy cost and external mechanical work

In figure 3.7 total energy cost C^T (full circles: •) is plotted as a function of the body mass of each subject. The regression line (thick-line) is described by:

$$C^T = 4.083 \cdot M - 11.024 \qquad (3.9)$$

(n=25, R^2=0.96, p<0.001).

Total external mechanical work W_{ext}^T (empty circles: ○) is also reported in figure 3.7, the corresponding equation (dotted-line) being described by:

$$W_{ext}^T = 1.712 \cdot M + 11.907 \qquad (3.10)$$

(n=25, R^2=0.84, p<0.001).

These data show that mean C^T and W_{ext}^T of obese subjects were 114.2% and 94.8% higher (p<0.001) than those of normal weighted group (see table 3.2).

3.4.3 Mass-specific energy cost and external mechanical work

In figure 3.8 mass-specific energy cost C (full circles: ●) is plotted as a function of the body mass M of all the subjects. The regression between the two variables (thick line) is described by:

$$C = 0.002 \cdot M + 3.729 \qquad (3.11)$$

(n=25, R2 =0.05, p=0.841), showing that no relationship exists between C and M. In addition, mean C of the obese subjects was not significantly different than that of the normal weight group (p=0.121, see table 3.2).

Mass-specific external mechanical work W_{ext} (empty circles: ○) is also plotted as a function of body mass M, in Figure 3.8. As for C, there is no relationship between W_{ext} and M, the regression line being described by:

$$W_{ext} = -0.001 \cdot M + 1.963 \qquad (3.12)$$

(n=25, R^2=0.01, p=0.962). In addition, W_{ext} was not significantly different (p=0.556) between obese and normal weight groups (table 3.2).

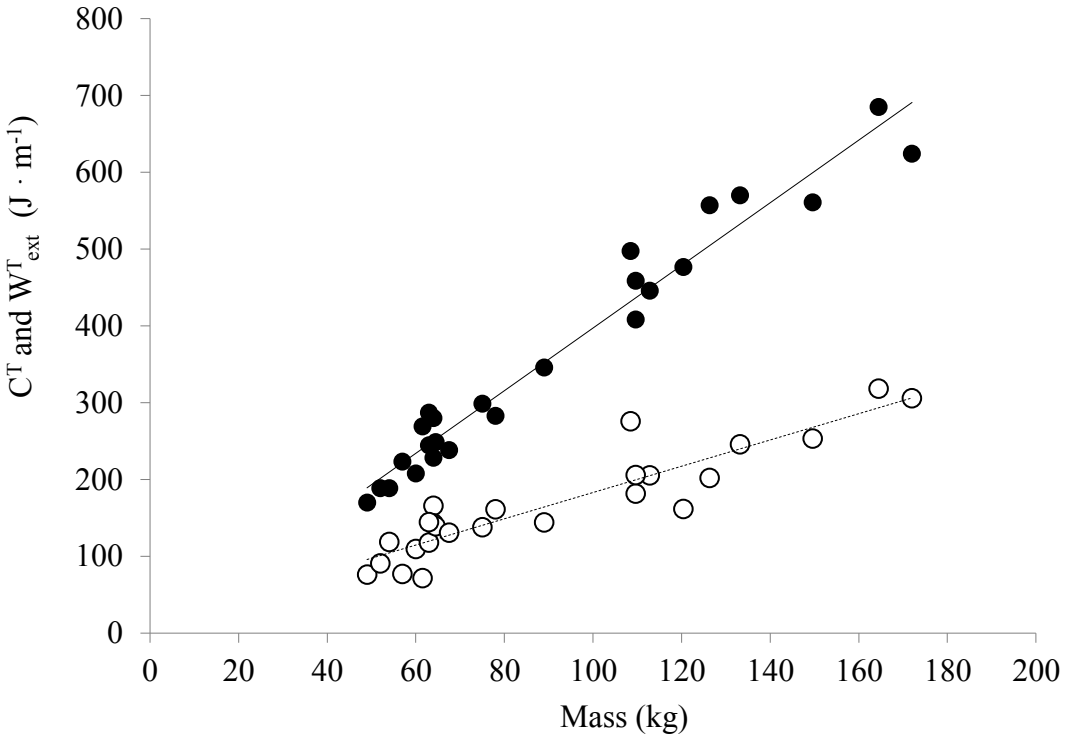

Figure 3.7 - Total energy cost of running (●: C^T, J·m-1) and external mechanical work (○: W_{ext}^T, J·m^{-1}) as a function of the overall body mass of the subject. Linear regression for C^T is described by: $C^T = 4.083 \cdot M - 11.024$ (n=25, R^2=0.96, p<0.001); linear regression for W_{ext}^T is described by $W_{ext}^T = 1.712 \cdot M + 11.907$ (n=25, R^2=0.84, p<0.001).

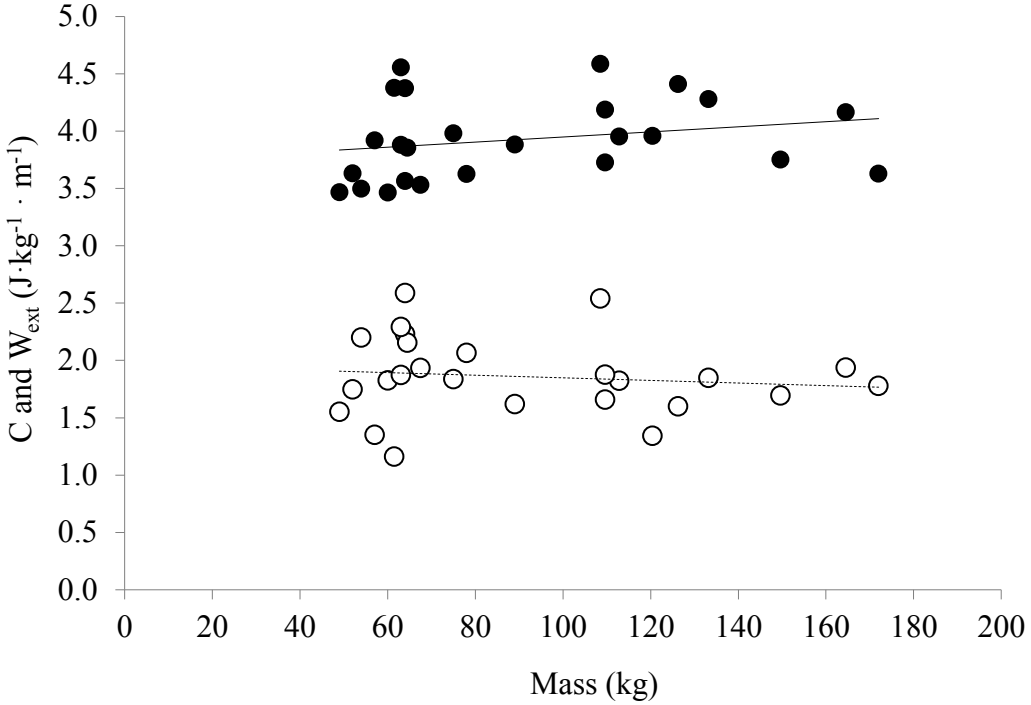

Figure 3.8 - Energy cost of running (●: C, J·kg^{-1}·m^{-1}) and external mechanical work (○: W_{ext}, J·kg^{-1}·m^{-1}) as a function of the overall body mass of the subject. Linear regression for C is described by : $C = 0.002 \cdot M + 3.729$, (n=25, R^2 =0.05, p=0.841); linear regression for W_{ext} is described by $W_{ext} = -0.001 \cdot M + 1.963$ (n=25, R^2=0.01, p=0.962)

3.4.4 Efficiency

In figure 3.9, efficiency η is plotted as a function of body mass. Since both C and W_{ext} are independent of body mass M, it necessarily follows that η is also independent of M: the equation of the regression line being

$$\eta = -0.062 \cdot M + 53.329 \qquad (3.13)$$

(n=25, R^2=0.05, p=0.838). In addition mean η was not significantly different (p=0.238) between obese and normal weight groups (table 3.2).

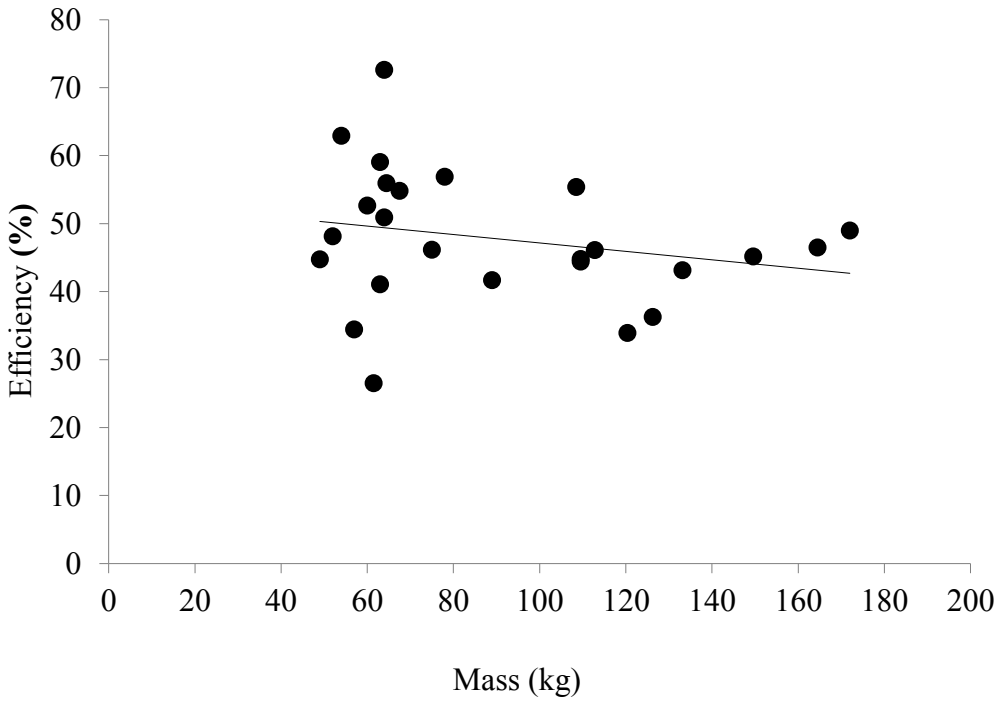

Figure 3.9 - Efficiency (%) as a function of the overall body mass M of the subject. Linear regression for efficiency is: $\eta = -0.062 \cdot M + 53.329$ (n=25, R^2=0.05, p=0.838).

	Obese (n=10)		Normal weighted (n=15)		p
C^T ($J \cdot m^{-1}$)	528.3 ± 86.3	[408.4 - 685.1]	246.7 ± 47.9	[169.8 - 345.6]	0.001
C ($J \cdot kg^{-1} \cdot m^{-1}$)	4.063 ± 0.314	[3.628 - 4.584]	3.839 ± 0.357	[3.463 - 4.556]	0.121
RER	0.92 ± 0.03	[0.88 - 0.98]	0.90 ± 0.06	[0.82 - 0.99]	0.201
W_{ext}^T($J \cdot m^{-1}$)	235.4 ± 52.8	[161.6 - 318.4]	121.7 ± 30.8	[71.4 - 165.6]	0.001
W_{ext} ($J \cdot kg^{-1} \cdot m^{-1}$)	1.808 ± 0.346	[1.342 - 2.539]	1.894 ± 0.378	[1.160 - 2.587]	0.556
Efficiency (%)	44.5 ± 6.0	[33.9 - 55.4]	49.9 ± 11.5	[26.7 - 72.6]	0.238

Table 3.2 - Physiological responses to running on treadmill C: energy cost of running; RER: respiratory exchange ratio at steady state running at 2.2 $m \cdot s^{-1}$ calculated as $VCO_2 \times VO_2^{-1}$; W_{ext}: external mechanical work; p: Significance by Student's t-test. All values are mean and standard deviation (SD). Minimum and maximum values in brackets

3.5 Discussion

The results of the present study show that mass-specific C and W_{ext} and, as a consequence, also the efficiency η are independent of the overall mass of the subjects.

3.5.1 Mass-specific energy cost and external work are independent of mass

At variance with the data collected by Heglund et al. (1982a, b) on birds and mammals, mass-specific energy cost of running (C) is independent of the overall mass of the subject. This is not surprising since the birds and mammals measured by Heglund et al. belonged to various species and, along with mass, numerous features differed substantially among them (overall dimensions, tissues, motor strategies, and so on). These differences are the result of millions of years of natural selection and differentiation among species. On the contrary, all subjects tested in this study belong to one species and they all share the same general body

structures, differing mainly in terms of FM. Hence mass alone does not seem to be a determinant for C.

Remarkably, Griffin et al. (2004) and Langman et al (2012) obtained comparable results when measuring mass-specific cost of transport in horses (*Equus caballus*)and in african elephants (*Loxodonta africana)* of different sizes (see figure 3.10): within the same species the cost of transport C remains the same, regardless of body mass.

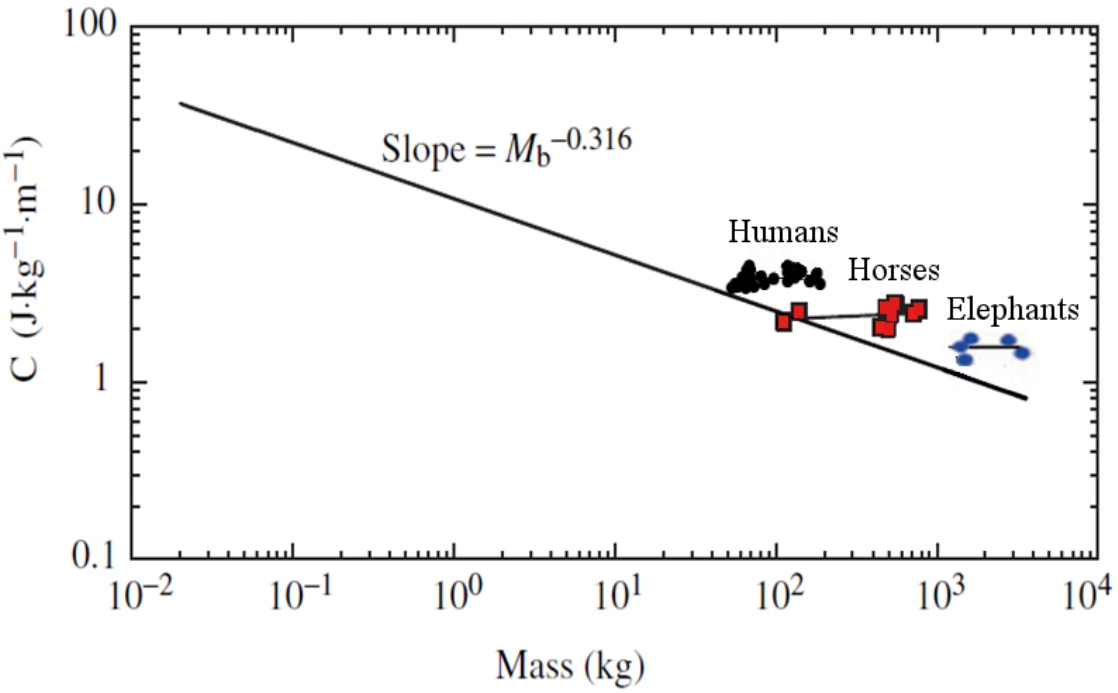

Figure 3.10 – Energy cost C of humans ($\propto M^{0.051}$), horses ($\propto M^{0.039}$, Griffin et al. 2004) and elephants ($\propto M^{0.007}$, Langman et al. 2012) of different masses. Within the same species, the allometric law $C = 10.71 \cdot M^{-0.316}$ does not apply.

These results seem to be in contrast with the data obtained by Bourdin et al. (1993), who analyzed the cost of running of young basketball players and middle-distance runners, showing that C was negatively correlated with body height and mass, the latter being the most important contributor. However, the lighter subjects analyzed by Bourdin et al. were very young (12.2 ± 1.9 and 14.2 ± 0.3 years, for girls and boys, respectively) compared to our group (18.2 ± 7.8 years)

and, as reported by the same authors, as well as by Sjödin and Svedenhag (1992), age plays a role in determining C.

Indeed, C ($J \cdot kg^{-1} \cdot m^{-1}$) decreases with age from a value of about 8.15 at age 4–6 to 5.02 at age 7–11, to 4.39 at 15 to about 3.97 at 20 (Daniels et al. 1978; MacDougal et al. 1983; Maliszewski and Freedson 1996; reviewed by di Prampero 2008). However, all our subjects were older than 16 years, in which case changes in C with age are negligible. Moreover, the subjects' mass range in Bourdin et al. 1993 study (23–82 kg) and Sjödin and Svedenhag (1992) study (35–66 kg) was small compared to ours (52–172 kg).

In another study, Bourdin et al. (1995) added an external load (9.3 % of body mass) to 10 male runners, finding that net Cr and W_{ext} per kg of total mass were significantly reduced. They explain the reduction of C as a consequence of the reduction in W_{ext}: a subject carrying a load modifies his/her motor strategies in order to reduce the overall external work, thereby reducing mass-specific C. Indeed Askew et al. (2011) find that an external added-mass (30–50 kg medieval armors) increases net C, both in walking and running, suggesting that if the added-mass if not only placed on the shoulders, the internal work needed to swing the limbs with added-mass plays a major role in determining the increase of C. On the contrary, carrying loads on the head leads to a significant reduction in the mass specific energy cost of walking in African women (Maloiy et al. 1986).

At variance with the results of these studies on the relationship between C and total mass, measurements made by Ferretti et al. (1991) on running pygmies (body mass 57.2 ± 4.8 kg) evidenced a C of 3.3 $J \cdot kg^{-1} \cdot m^{-1}$, significantly lower than the value predicted by allometric equations (4.4 $J \cdot kg^{-1} \cdot m^{-1}$). The same authors state that their findings "challenge the theory of physical similarity as applied to animal locomotion".

Previous studies on walking humans by Browning et al. (2009), Peyrot et al. (2009) and Malatesta et al. (2009) reported that W_{ext} does not vary with mass. Our data indicate that also for running W_{ext} is independent of the overall mass of the subject, a fact also reported by Heglund, Taylor et al. (1982) for animals. This may indicate that when the ''added mass'' is FM, i.e., the consequence of months or even years of excessive food intake, an obese subject can ''train'' as his/her mass increases, maintaining the same motor strategies adopted by normal-weighted subjects, i.e., developing the same W_{ext} and therefore C. Heglund, Taylor et al. (1982) reported that also in animals of different species W_{ext} is independent of the overall mass. At variance with W_{ext}, the mass-specific energy cost of running (C) decreases with the overall mass, a fact that may indicate a better motor strategy in the heavier animal species and/or a greater fractional recovery of elastic energy.

3.5.2 Efficiency

Total mechanical work (W_{tot}), as given by the sum of W_{ext} and W_{int} , should be considered to calculate the overall ''true'' efficiency. As mentioned above, however, we calculated only the ''external'' efficiency and, since W_{ext} is less than W_{tot}, the overall ''true'' efficiency is greater than external efficiency, which can therefore be considered a minimal value.

In both groups this ''minimal efficiency'' is substantially larger than the maximal efficiency of concentric muscle contractions which can be expected to be on the order of 25–30 %. This finding suggests that a large amount of elastic energy storage and release occurs in both obese and normal-weighted subjects, thus reducing the metabolic energy requirements (Cavagna et al. 1977).

3.5.3 Methodological limitations

The position of the CoM depends on the relative position of the limbs, trunk, and head. Even so, we assumed that the CoM is placed at the pelvic center and that its position does not vary as the subject moves the limbs while running. Previous tests in our laboratory allowed us to compare the position of the CoM calculated by means of a 15 segments model (Hanavan, 1964) with the approximated "3 points" model used in this study on the same subject, in particular we used the following measure:

$$diff = z_1 - z_2 \qquad (3.14)$$

where z_1 is the vertical position of the CoM calculated by means of the 15 segments model, z_2 is the vertical position of the CoM calculated by means of the 3 points model and $diff$ is their difference (measured in m). As reported in figure 3.6, at 2.2 m $\cdot$ s^{-1} the value is always comprised between -0.014 m and +0.011 m, showing therefore a good agreement between the two models.

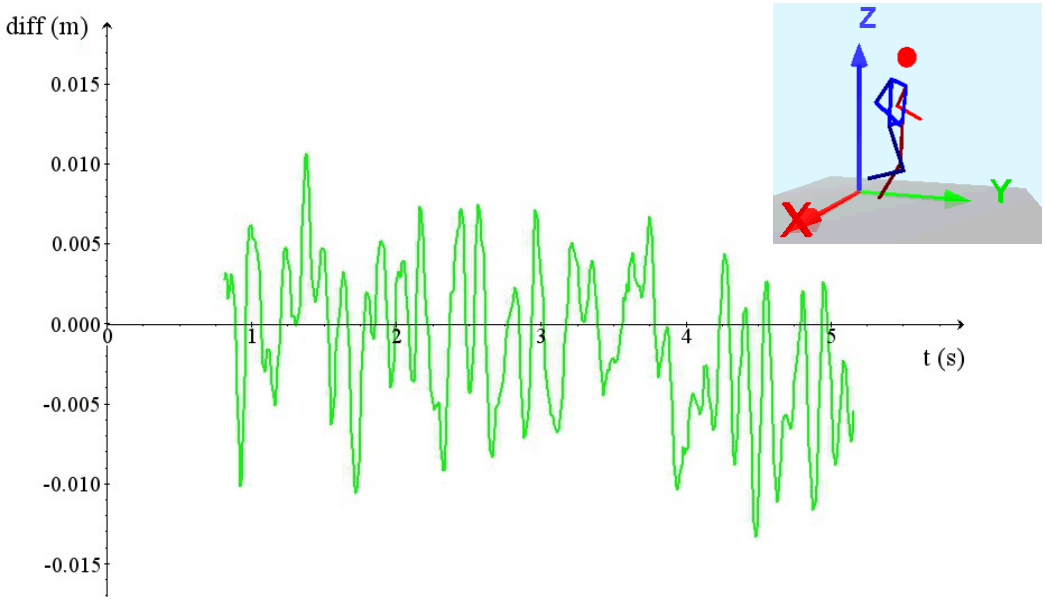

Figure 3.6 - Difference (diff, in m) in the vertical position of the CoM between the 15 segments Hanavan model and the 3 point model utilized in this research. The speed of the subject was 2.2 m·s^{-1}. In the upper right corner a representation of the reconstructed subject is shown.

The assumption of placing the CoM at the pelvic center was validated by Myers and Steudel (1985) and Bourdin et al. (1995); moreover, the values of W_{ext} calculated here are ~20 % higher than data obtained in previous studies with force platform methods (Cavagna et al.1976, 2008, Willems et al. 1995), considered as ''gold-standard''.

This difference can be due to the fact that our subjects ran on a treadmill, compared with indoor tracks used by the cited authors; thus the vertical oscillations of the treadmill may have increased the calculated W_{ext}. The higher W_{ext} may also be explained by the tilting of the trunk, which might overestimate the kinetic forward work evaluated by the displacements of the single point at the center of the pelvis (Bourdin et al. 1995).

Internal mechanical work W_{int}, i.e., the work done to accelerate and rotate the limbs relative to the CoM, was not considered in this study, even if plays a role in the overall energy consumption. However, its contribution at low speeds is small as compared to W_{ext} at least in normal weighted subjects; (e.g., Willems et al. (1995) showed that, at about 2 $m \cdot s^{-1}$, W_{int} is about one-third of W_{ext}). On the other hand, obese subject have relatively heavier limbs (e.g., Browning et al. 2007, 2006) and this may imply higher W_{int} than in normal-weighted subjects.

3.6 Conclusions

As both mass-specific C and W_{ext} and, as a consequence, also η are independent of the overall mass of the subjects, the results of this study strongly suggest that the elastic tissues of obese subjects can adapt (e.g., thickening) to the increased mass of the body, thus maintaining their ability to store elastic energy, at least at 2.2 $m \cdot s^{-1}$ speed, at the same level as the normal-weighted subjects.

In conclusion, it is tempting to suggest that the constancy of C in obese subjects, rather than its decline with increasing body mass, is a maladaptive response. Indeed it can be calculated that C in our most obese subject (172 kg), where it follows the allometric law applying to bipedal mammals (Taylor 1977), ought to be 3.3 $J \cdot kg^{-1} \cdot m^{-1}$, i.e., about 9 % smaller as compared to the observed 3.7 $J \cdot kg^{-1} \cdot m^{-1}$. This maladaptive response is partially compensated for by the above-mentioned response of the elastic tissues of the body, the effect of which is to maintain the mass-specific energy cost of running to the values applying to a normal-weighted subject.

3.7 References

Askew GN, Formenti F, Minetti AE. (2011) Limitations imposed by wearing armour on medioevals soldiers locomotor performance. *Proc. R. Soc. B.* (PMID: 21775328)

Bourdin M, Pastene J, Germain M, Lacour JR. (1993) Influence of training, sex age and body mass on the energy cost of running. *Eur. J. Appl. Physiol.* 66: 439-44

Bourdin M, Belli A, Arsac LM, Bosco C, Lacour JR. (1995) Effect of vertical loading on energy cost and kinematics of running in trained male subjects. *J. Appl. Physiol*. 79(6): 2078-85

Browning RC, Baker EA, Herron JA, Kram R (2006) Effects of obesity and sex on the energetic cost and preferred speed of walking. *J. Appl. Physiol.* 100(2): 390-8

Browning RC, Kram R (2007) Effects of obesity on the biomechanics of walking at different speeds. *Med Sci Sports Exerc.* 39(9): 1632-41

Browning RC, McGowan CP, Kram R. (2009) Obesity does not increase external mechanical work per kilogram during walking. *J. Biomech.* 42: 2273-8

Brueckner JC, Atchou G, Capelli C, Duvallet A, Barrault D, Jousselin E, Rieu M, di Prampero PE. (1991) The energy cost of running increases with the distance covered *Eur. J. Appl. Physiol* 62: 385-389.

Cacciari E, Milani S, Balsamo A, Spada E, Bona G, Cavallo L, Cerutti F, Gargantini L, Greggio N, Tonini G, Cicognani A. (2006) Italian cross-sectional growth charts for height, weight and BMI (2 to 20yr). *J. Endocrinol. Invest.* 29: 581-93.

Cavagna GA, Heglund NC, Taylor CR. (1977) Mechanical work in terrestrial locomotion: two basic mechanisms for minimizing energy expenditure. *Am J Physiol*. 233(5): R243-61

Cavagna GA, Kaneko M. Mechanical work and efficiency in level walking and running. (1977) *J. Physiol.* 268: 467-81

Cavagna GA, Legramandi MA, Peyrè-Tartaryga LA. (2008) Old men running: mechanical work and elastic bounce. *Proc. R. Soc. B*. 275: 411-8

Cavagna GA, Thys H, Zamboni A. (1976) The sources of external work in level walking and running. *J. Physiol*. 262: 639-57

Daniels J, Oldridge N, Nagle F, White B. (1978) Differences and changes in VO2 among young runners 10 to 18 years of age. *Med Sci Sports Exerc.* 10: 200-3

Diss CE (2001) The reliability of kinetic and kinematic variables used to analyse normal running gait. *Gait Posture.* 14(2): 98-103

di Prampero PE (1986) The energy cost of human locomotion on land and in water. *Int J Sports Med* . 7(2): 55-72

di Prampero PE (2008) In "Physiological Bases of Human Performance during Work and Exercise" NAS Taylor, H Groeller, eds Section 3 Age - Introduction "Physical activity in the 21st century: challenges for the young and old. PP 267 – 273

Fedak MA, Heglund NC, Taylor CR. (1982) Energetics and mechanics of terrestrial locomotion. II. Kinetic energy changes of the limbs and body as a function of speed and body size in birds and mammals. *J. exp. Biol.* 97, 23-40

Ferretti G, Atchou G, Grassi B, Marconi C, Cerretelli P. (1991) Energetics of locomotion in African Pygmies. *Eur. J. Appl. Physiol.* 62: 7-10.

Gullstrand L, Halvorsen K, Tinmark, Eriksson M, Nilsson J. (2009) Measurements of vertical displacement in running, a methodological comparison *Gait Posture* 30: 71-75

Heglund NC., Cavagna GA, Taylor CR. (1982) Energetics and mechanics of terrestrial locomotion. III. Energy changes of the centre of mass as a function of speed and body size in birds and mammals. *J. exp. Biol.* 97, 41–56

Heglund NC, Fedak MA, Taylor CR, Cavagna GA. (1982) Energetics and mechanics of terrestrial locomotion. IV. Total mechanical energy changes as a function of speed and body size in birds and mammals. *J. exp. Biol.* 97, 57–66

Lukaski HC, Bolonchuk WW, Hall CB, Siders WA. (1986) Validation of tetrapolar bioelctrical impedance to assess human body composition. *J Appl Physiol*. 60: 1327-32

MacDougal JD, Roche PD, Bar-Or O, Moroz JR. (1983) Maximal aerobic capacity of Canadian School children: prediction based on age relatd oxygen cost of running. *Int J Sports Med*. 4: 194-198

Malatesta D, Vismara L, Menegoni F, Galli M, Romei M, Capodaglio P. (2009) Mechanical external work and recovery at preferred walking speed in obese subjects. *Med. Sci. Sports Exerc.* 41(2): 426-34

Maliszewski AF, Freedson PS. (1996) Is running economy different between children and adults? *Pediatirc Exercise Science*. 8: 351 - 360

Maloiy GM, Heglund NC, Prager LM, Cavagna GA, Taylor CR. (1986) Energetic cost of carrying loads: have African women discovered an economic way? *Nature.* 319: 668-9

Margaria R, Cerretelli P, Aghemo P, Sassi G. (1963) Energy cost of running. *J Appl Physiol.* 18: 367-370

Myers MJ, Steudel K. (1985) Effect of limb mass and its distribution on the energetic cost of running. *J Exp Biol.* 116: 363-73

Nolan L, Patritti BL, Simspon KJ. (2006) A Biomechanical Analysis of the Long-Jump Technique of Elite Female Amputee Athletes. *Med Sci Sports.* 38(10): 1829-1835

Peyrot M, Thivel D, Isacco L, Morin JB, Duche P, Belli A. (2009) Do mechanical gait parameters explain higher metabolic cost of walking in obese adolescents? *J. Appl. Physiol.* 106(6): 1763-70

Taylor CR (1977). In "Scale Effects in Animal Locomotion", T.J. Pedley, editor, Academic Press, London, PP. 127 - 141

Taylor CR, Heglund NC, Maloiy GM. (1982) Energetics and mechanics of terrestrial locomotion. I. Metabolic energy consumption as a function of speed and body size in birds and mammals. *J. exp. Biol.* 97: 1-21

Willems PA, Cavagna GA, Heglund C. (1995) External, internal and total work in human locomotion. *J Exp Biol*. 198 (Pt 2): 379-393

Web sites

"Kelvin (4-wire) resistance measurement"
<http://www.allaboutcircuits.com/vol_1/chpt_8/9.html>

4. Part IIa: Optimal starting block configuration in sprint running; a comparison of biological and prosthetic legs

4.1 Introduction

In both the Olympic and Paralympic Games, the start of the 100m event is very important to overall performance. In the Olympic 100m, the start comprises ~5% of the total race time (Harland and Steele, 1997) and athletes need 30-40m to reach their maximum speed (di Prampero et al. 2004). However, for athletes with unilateral and bilateral transtibial amputations (T43/T44 classification) in the Paralympic 100m, it is apparent that the acceleration phase is much longer, particularly for bilateral amputees. Slower accelerations likely reflect the lack of ankle muscle power combined with the compliance of the leg prosthesis. However, there are no published studies regarding the sprint start biomechanics of athletes with leg amputations. Thus, our overall goal was to quantify and better understand how leg prostheses affect start performance.

In sprint running races, it is mandatory for athletes to use starting blocks (IAAF Competition Rules). Each athlete must position their feet against two adjustable plates anchored to the track. One foot is placed on the front block, typically ~0.5m behind the start line, and one foot is placed on the back block, ~0.8m behind the start line (Mero, 1988; Gutiérrez-Dávilla et al. 2006). The left/right foot positions and distances from the start line are based on the athlete's preference. Athletes fine-tune their starting block positions mostly by trial-and-error in the initial years of practice and typically converge on a final configuration, with little or no changes throughout the rest of their career (Eikenberry et al. 2008). Although non-amputee athletes have nearly symmetric legs, they tend to place their dominant leg on the front block (Newton et al. 2006). Further, Fortier

et al. (2005) has shown that non-amputees generate greater forces and impulses with their front leg during a sprint start.

In contrast, the legs of athletes with unilateral leg amputations are asymmetric. Their unaffected leg (UL) has both active (muscle) and passive-elastic (tendon) components; whereas the affected leg (AL) of high caliber athletes is typically fitted with a J-shaped carbon-fiber prosthesis that is elastic but completely passive. These lower-leg running specific prostheses (RSP) are designed to store elastic energy during the first half of the contact phase, and return it during the second half of the contact phase. But, when using starting blocks, these athletes are not able to utilize the elastic energy storage and return of an RSP, because in the "set" position, the athlete must be still and no bouncing is allowed (IAAF Competition Rules). Therefore, the force exerted by the affected leg (AL) onto the starting block is solely provided by the remaining proximal muscles. At constant speeds, sprinters using RSPs generate lower forces with their affected leg (AL) compared to their unaffected leg (UL) (Grabowski et al. 2010, see figure 4.1).

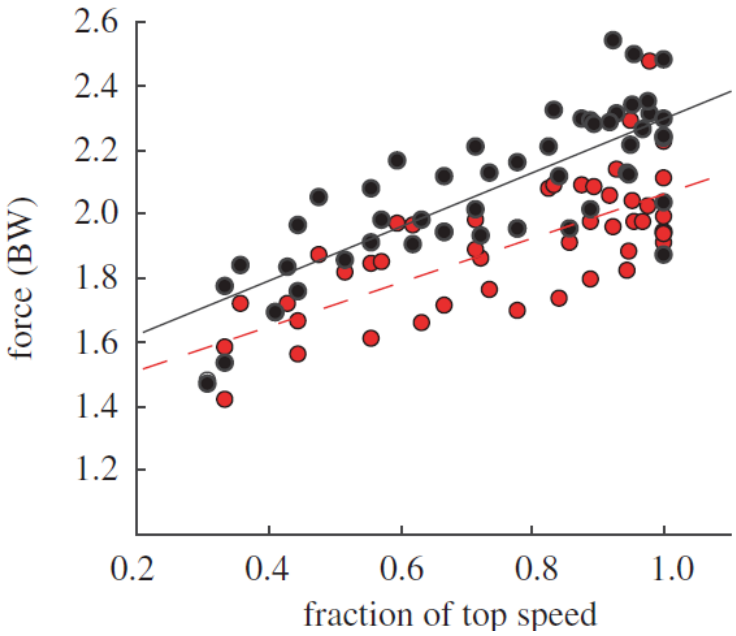

Figure 4.1 – Vertical ground reaction forces (expressed as a function of body weight BW) in sprinters with unilateral transtibial amputation. Filled black circle: UL, filled red circle: AL. (Grabowski et al. 2010)

However, there have been no published studies that have quantified the forces exerted on the starting blocks by sprinters using an RSP.

Horizontal acceleration, a metric that quantifies a sprint start, is the result of the horizontal forces applied on the blocks. Thus, we reasoned that to optimize start performance, an athlete with a unilateral leg amputation should start with their unaffected leg in front, assuming the UL can generate greater force. Indeed, video recordings of sprint athletes with unilateral transtibial amputations competing in the 100m and 200m men's and women's T43/T44 finals of the 2008 Beijing Paralympics reveal that 13 of 17 adopted this configuration (www.youtube.com). Similarly, video recordings of the 2012 London Paralympics reveal that 19 of 22 athletes placed their UL on the front block (www.youtube.com, see figure 4.2). Can this strong preference among Paralympic athletes be supported by biomechanical data?

Figure 4.2 – Men's 200m T43-T44 final, London 2012 Paralympic Games. The athlete in lane 8 places his unaffected leg on the front block, while the athlete in lane 9 places his affected leg on the front block. (http://www.youtube.com/watch?v=A9Wlp1sTnoY)

4.2 Aims of the study

The aim of the present study was to measure the effect of starting block configuration on starting performance of both non-amputee sprinters and athletes with unilateral transtibial amputations. We hypothesized that sprinters with unilateral transtibial amputations using a starting block configuration with the UL in front would have better acceleration out of the blocks compared to using the configuration with the AL in front.

4.3 Research design and methods

4.3.1 Subjects

A total of 16 subjects participated in this study: 7 (6 males and 1 female) were non-amputee sprinters and 9 (7 males and 2 females) were sprinters with a unilateral transtibial amputation (table 4.1). All subjects gave their written informed consent before participating in this study as per the University of Colorado Institutional Review Board.

4.3.2 Experimental design

Each subject performed a total of 6 starts, alternating between their usual and unusual starting block configurations. The initial configuration was randomized. For the unusual blocks configuration, front and back blocks were switched while maintaining the same relative distance from the starting line. For each start, the investigator gave the standard verbal commands used in sprint races: “on your marks” and “set”. After the subject assumed the set position, a computer-generated audio gun shot was provided by a nearby computer speaker. The audio signal also triggered force data collection. Each subject was instructed to run as fast as possible to a line placed 5m from the start. Between each trial, 8 minutes of rest were enforced to decrease the potential for fatigue.

Each athlete positioned their front and back blocks on two separate force platforms (LG6-4-2000, Advanced Mechanical Technology, Watertown, MA, USA) located underneath a runway covered with a rubber mat, which allowed each athlete to use their own spiked shoes. Each subject placed his/her feet against the blocks and his/her hands on a wide (1.22 m x 0.6 m) “winged” plate secured on top of the front force platform (Fig. 4.3). The winged plate was wider than the

force platform, and allowed us to measure the combined forces exerted by the front foot and both hands. We measured the forces exerted by the back foot from a plate secured on top of the back force platform. We sampled the force signals at 1000Hz via a data acquisition device (NI USB-6009, National Instruments Corp., USA) and a custom program (LabView, National Instruments Corp., USA). Then, we filtered the data with a 4th order Butterworth low-pass filter with a cut-off frequency of 30Hz. To obtain the total force exerted, we summed the signals from the front and back force platforms.

We used a second custom program (Matlab) to analyze the data. We identified the actual start of the push-phase for each subject, (defined as the instant when the total horizontal force exceeded a threshold of 5N) and the end of the push-phase, (defined as the instant when the total horizontal force crossed the 0N value). We calculated the reaction time as the interval between the start audio signal and the start of the push-phase (see Fig. 4.4).

	Subject	Sex (M/F)	Age (years)	Height (m)	Mass (kg)	100m PR (s)	Usual front leg (L/R)	RSP Model
Non amputee	1	M	18	1.73	66.7	11.58	L	
	2	M	18	1.76	81.8	11.70	L	
	3	M	44	1.75	75.1	11.80	L	
	4	M	33	1.75	65.8	12.22	L	
	5	M	45	1.65	68.1	12.42	L	
	6	M	19	1.82	96.0	12.96	L	
	7	F	24	1.65	74.1	14.75	L	
Average ± S.D.			30.3 ± 12.3	1.73 ± 0.06	75.4 ± 10.7	12.49 ± 1.11		
Amputee	1	M	33	1.91	112.3	12.14	L (UL)	Ottobock Sprinter
	2	M	24	1.75	74.5	12.40	L (UL)	Ossur Cheetah
	3	M	28	1.88	79.6	12.60	L (UL)	Ossur Flexfoot Sprint
	4	M	18	1.78	92.2	14.50	R (UL)	Ossur Cheetah
	5	F	21	1.70	59.0	15.63	L (UL)	Ottobock Sprinter
	6	M	29	1.83	73.9	11.90	R (AL)	Ottobock Sprinter
	7	M	22	1.77	73.9	12.60	R (AL)	Ottobock Sprinter
	8	F	27	1.70	64.2	13.61	L (AL)	Ottobock Sprinter
	9	M	28	1.70	60.7	26.33 (200m)	R (AL)	Ossur Cheetah
Average ± S.D.			25.6 ± 4.7	1.78 ± 0.08	76.7 ± 16.8	13.17 ± 1.31		

Table 4.1 - Subject characteristics. Demographic and anthropometric variables and 100m personal records (PR) of non-amputee and amputee subjects. For the amputee group, The front leg for the usual configuration is indicated for non-amputees and amputees (AL is the affected leg and UL is the unaffected leg). Each amputee subject's running specific prosthesis (RSP) model is reported. Average values ± standard deviations are reported for both groups.

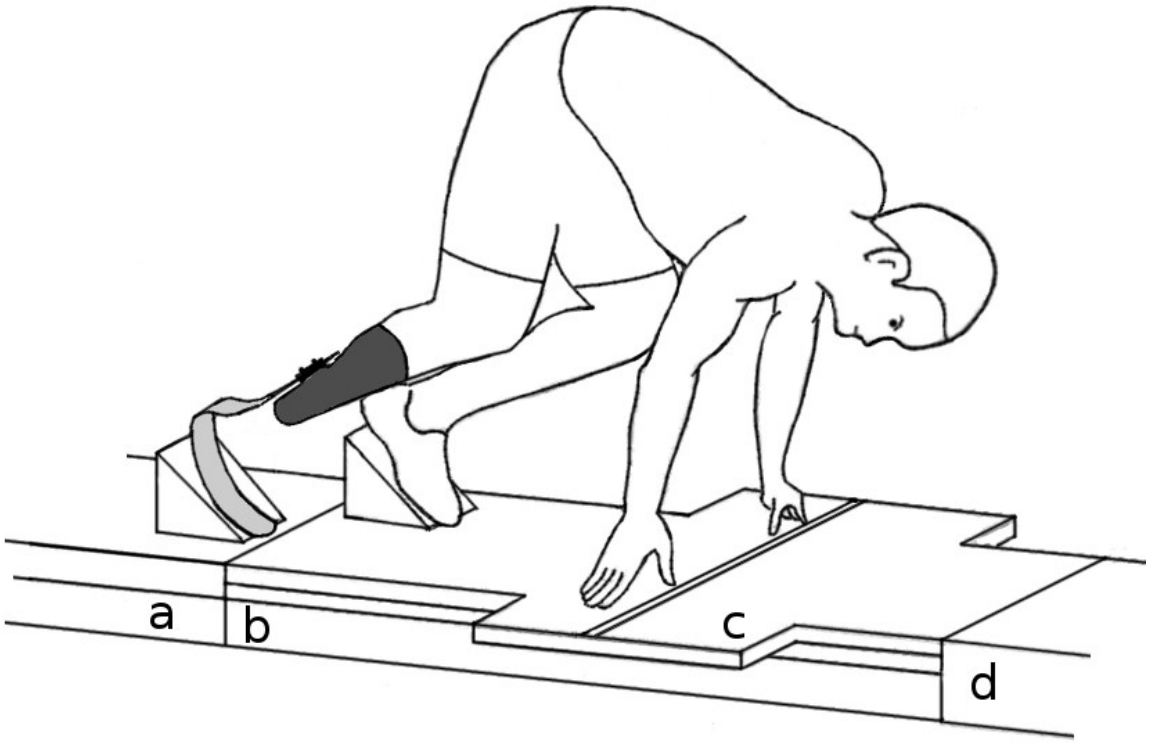

Figure 4.3 - Experimental set-up of a starting blocks configuration. This athlete has his back affected leg, with his RSP, on force platform "a", his front unaffected leg and hands on the "winged" plate "c", secured to force platform "b". After the start, he runs as fast as possible on the elevated runway "d".

Various authors have proposed different measures of start performance, ranging from horizontal and total force applied on the starting blocks (Mero, 1988), delay between the end of the rear and front force offset (Fortier et al. 2005) and net horizontal external power (Bezodis et al. 2010). There is no universally agreed upon metric for start performance. We calculated the following parameters to better understand start performance: reaction time (s), push-time (s), mean and peak total (front+back) resultant force normalized to body weight (BW), mean push angle (degrees), mean and peak mass-specific total horizontal power ($W \cdot kg^{-1}$), horizontal impulse ($BW \cdot s$), horizontal velocity at the end of the push-phase ($m \cdot s^{-1}$), mean horizontal acceleration of the push-phase ($m \cdot s^{-2}$), front-leg and back-leg mean and peak horizontal force normalized to body weight (BW) and mass-specific mean and

peak power ($W \cdot kg^{-1}$) in the horizontal direction. More specifically, we calculated the back and front leg mean forces and powers over the relative push-phase of each leg, and calculated the total mean force and power over the entire push phase. We defined the mean push angle as the angle of the mean total resultant force vector with respect to horizontal.

4.3.3 Virtual athletes

For each amputee sprinter, we used data from their UL and AL to simulate their start mechanics as if they 1. had two unaffected legs ("a virtual non-amputee") or 2. had two affected legs ("a virtual bilateral amputee"). Given that each sprinter switched front and back legs in the usual and unusual block configurations, we generated a virtual non-amputee by summing the impulse of their UL when it was placed on the front block I_{UL}^{front} and the impulse of the UL when it was placed on the back I_{UL}^{back}:

$$I_{UL}^{total} = I_{UL}^{front} + I_{UL}^{back} \qquad (4.1)$$

Then, we divided the total impulse by the push-time(t_{push}) to obtain mean force ($F_{non\ amputee}$):

$$F_{non\ amputee} = \frac{I_{UL}^{total}}{t_{push}} \qquad (4.2)$$

We performed all calculations in both the horizontal (h) and vertical (v) directions, obtaining mean resultant force and push-angle. Lastly, we calculated the

mean horizontal acceleration by dividing the mean horizontal force by the body weight of each athlete:

$$a_h = {}^{F_h}/_{BW} \qquad (4.3)$$

We made the same calculations for the AL to simulate a virtual bilateral amputee (see figure 4.4).

We assumed that the body weight of the virtual non-amputee and virtual bilateral amputee was the same as the respective unilateral amputee, neglecting any mass differences between the UL and AL.

4.3.4 Statistical analysis

We checked the normality of the samples with the Shapiro-Wilk test and then used a paired samples t-test to assess the differences between usual and unusual configurations in both groups and between the UL and AL front leg configurations in the amputee group. A p value of less than or equal to 0.05 was accepted as significant.

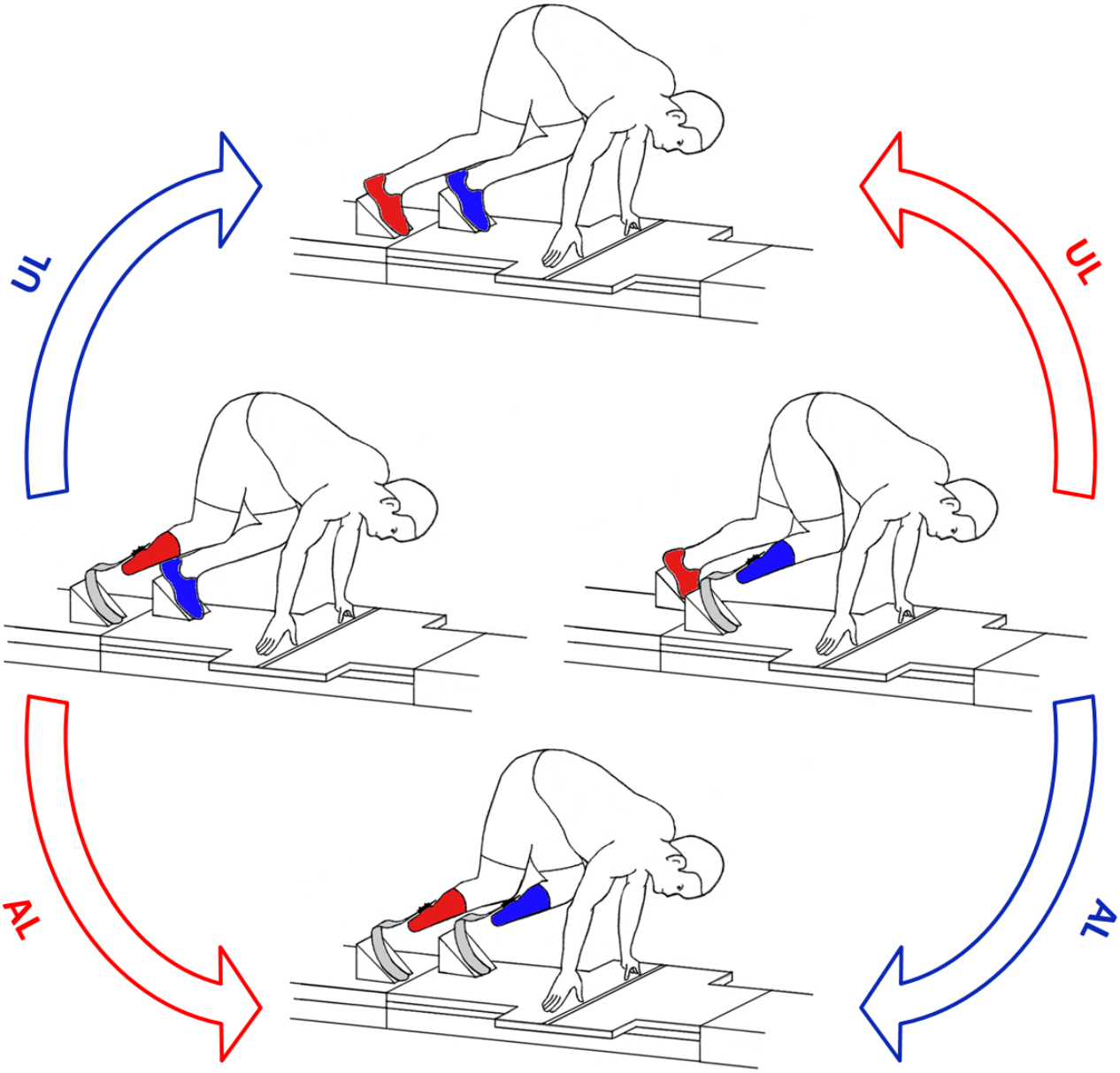

Figure 4.4 – Each sprinter switched front (blue) and back (red) legs in the usual and unusual block configurations (central panels). We generated the virtual non amputee by summing the contribution of the UL when it was placed on the front and on the back block (upper panel). We generated the virtual bilateral amputee by summing the contribution of the AL in the two configurations (lower panel).

4.4 Results

4.4.1 Reaction time and push time

We found no significant differences between or within groups for reaction times among the different configurations (Table 4.2). For the non-amputee sprinters, push-time was slightly but significantly shorter in the usual configuration compared to the unusual configuration (0.407 ± 0.035 vs. 0.416 ± 0.044 s, p=0.043, n=7). For the amputee sprinters, the push-times were not significantly different between usual and unusual configurations or between UL and AL in front configurations.

4.4.2 Total resultant forces and push angles

We found no differences in mean and peak total resultant forces and push-angles between the two configurations in the non-amputee sprinters (see figure 4.4 and table 4.2). However, we found that for sprinters with an amputation, the mean total resultant force was greater in the usual versus unusual configuration (1.37 ± 0.07 vs. 1.30 ± 0.10 BW, p=0.038, n=9), but found no differences in peak total resultant forces or push angles. When comparing the UL in front versus the AL in front configurations, we found that the mean total resultant force was significantly greater when the UL was placed in front (1.38 ± 0.06 vs. 1.30 ± 0.11 BW, p=0.015, n=9). However, the peak total resultant force was smaller for UL in front vs. AL in front configurations (2.10 ± 0.18 vs. 2.36 ± 0.21 BW, p=0.0010, n=9). Having the UL in front resulted in a more vertical mean push-angle compared to having the AL in front (59.4 ± 2.2 vs. 57.8 ± 2.7 deg, p=0.029, n=9).

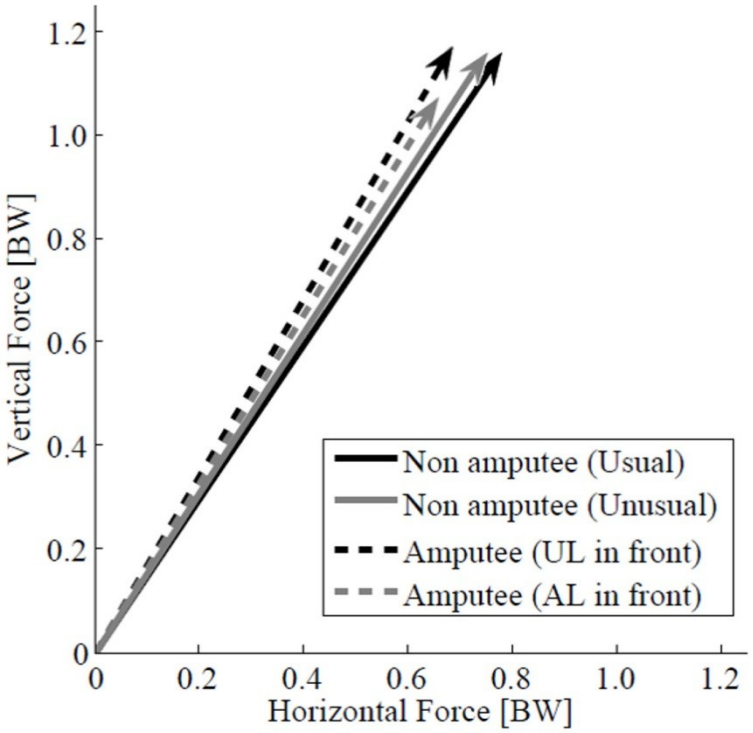

Figure 4.4 - Mean resultant force vectors (average values) for non-amputee (n=7) and amputee sprinters (n=9) in usual vs. unusual and affected leg (AL) vs. unaffected leg (UL) in front, respectively. There were no differences between conditions for non–amputee sprinters. Amputee sprinters with their UL in front developed more force (p=0.015) and directed it more vertically (p=0.029) compared to the configuration with their AL in front.

We found that there were greater differences between the UL in front vs. AL in front configurations, compared to the amputee sprinters' usual vs. unusual configurations. Therefore, the subsequent results section focuses only on the UL in front vs. AL in front for the amputee sprinters group.

4.4.3 Horizontal direction

4.4.3.1 Total (front + back) measurements

We found that the non–amputee sprinters had slightly but significantly greater mean total force in the horizontal direction for the usual vs. unusual configuration (0.78 ± 0.09 vs. 0.75 ± 0.09 BW, p=0.042, n=7). Therefore the mean horizontal acceleration was greater for the usual vs. unusual configuration (7.63 ± 0.91 vs. 7.39 ± 0.84 $m \cdot s^{-2}$,p=0.042, n=7). Between the usual vs. unusual configurations there were no differences in peak total force, power, final velocity nor in impulse at the end of push-time (see table 4.3 and figure 4.5).

We found that the amputee sprinters had significantly smaller peak total force in the UL in front compared to the AL in front configuration (1.12 ± 0.13 vs. 1.31 ± 0.18 BW, p=0.008, n=9) However, the mean total force, power, acceleration and final velocity data showed no significant differences between block configurations.

4.4.3.2 Single-leg measurements

As shown in Table 4.4, there were no statistically significant differences between the front and back leg in the usual and unusual configurations in the non-amputee sprinters, but all values in the usual configuration resulted in numerically better performance, except for front leg mean forces, which were equal in the two configurations.

The amputee sprinters had greater mean front leg force when the UL was in front (0.60 ± 0.13 vs. 0.52 ± 0.11 BW, UL in front vs. AL in front, respectively, p=0.016, n=9). However, the following key variables were superior for the AL in front configuration: mean back leg force (0.27 ± 0.13 vs. 0.38 ± 0.13 BW ,

p=0.025), mean back leg power (1.48 ± 1.04 vs. 2.44 ± 1.40 W/kg, p=0.048) and peak back leg power (3.53 ± 2.38 vs. 6.76 ± 3.16 W/kg, , p=0.017), all values refer to UL in front vs. AL in front respectively, n=9.

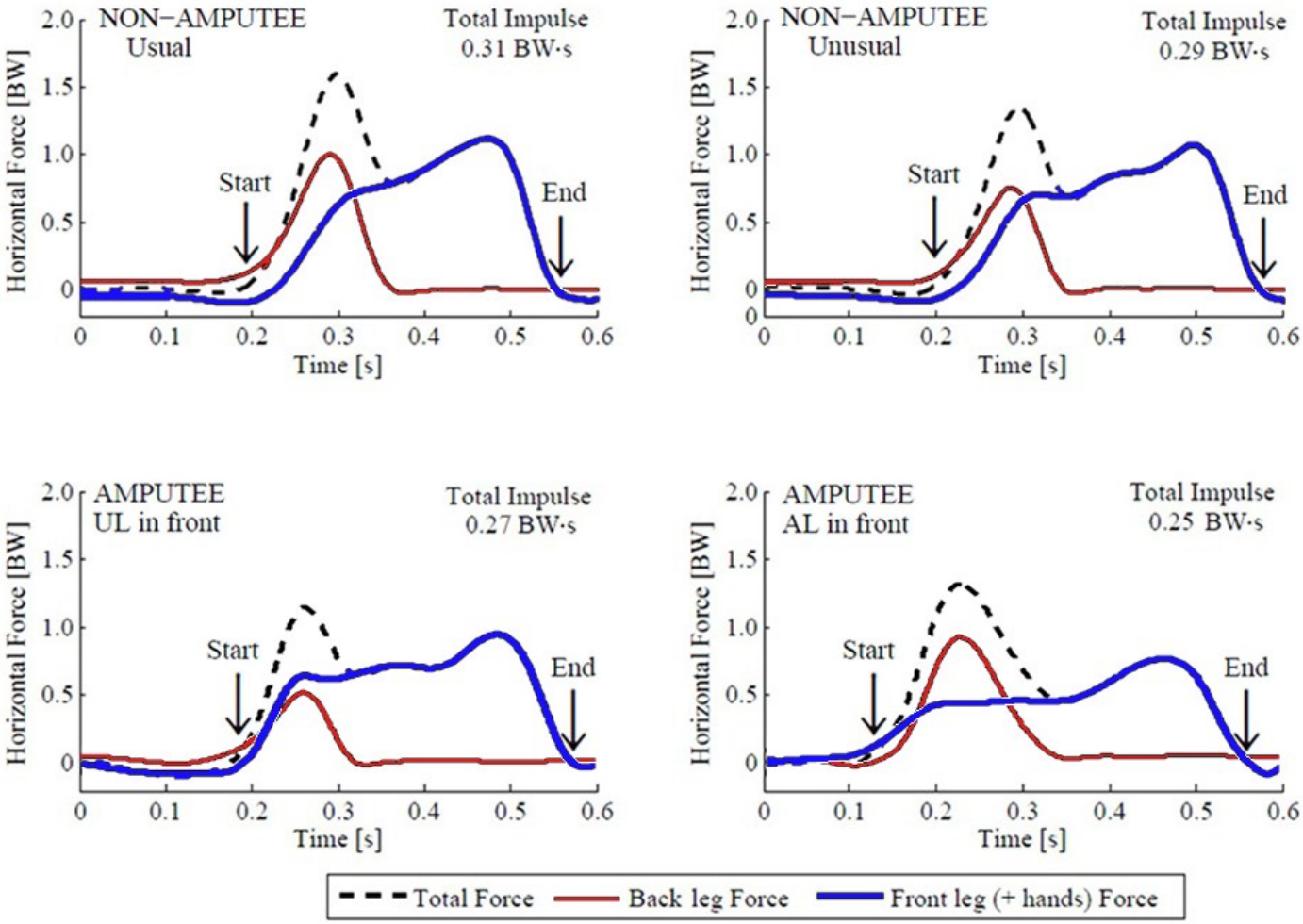

Figure 4.5 - Typical horizontal force traces for a non-amputee sprinter (upper panels) in the usual and unusual blocks configurations and for a sprinter with a unilateral transtibial amputation (lower panels) with the unaffected leg (UL) and affected leg (AL) on the front block: Time = 0 identifies the start signal, "Start" indicates the actual start (Horizontal Force > 5N), "End" indicates the end of the push-phase, the time between Start and End is the push time.

		Reaction Time (s)	Push time (s)	Mean Resultant Force (BW)	Peak Resultant Force (BW)	Mean Push angle (deg)
Non amputee (n=7)	Usual	0.155 ± 0.043	**0.407 ± 0.035**	1.40 ± 0.07	2.28 ± 0.21	55.9 ± 3.1
	Unusual	0.163 ± 0.036	**0.416 ± 0.044**	1.39 ± 0.07	2.30 ± 0.25	56.6 ± 3.0
Amputee (n=9)	Usual	0.173 ± 0.060	0.417 0.059	**1.37 ± 0.07**	2.26 ± 0.23	58.3 ± 3.2
	Unusual	0.188 ± 0.083	0.424 0.052	**1.30 ± 0.10**	2.21 ± 0.24	59.0 ± 1.6
Amputee (n=9)	UL in front	0.175±0.061	0.419 ± 0.046	**1.38 ± 0.06**	**2.10 ± 0.18**	**59.4 ± 2.2**
	AL in front	0.192±0.076	0.422 ± 0.059	**1.30 ± 0.11**	**2.36 ± 0.21**	**57.8 ± 2.7**

Table 4.2 - Reaction times, push times, mean and peak resultant forces, and mean push angles. Each value is reported as mean ± S.D. Highlighted gray indicates the value that results in the best performance between the two configurations. Statistically significant ($p<0.05$) differences between the 2 configurations within each group are highlighted in **bold**.

		Horizontal					
		Mean Total Force (BW)	Peak Total Force (BW)	Mean Total Power ($W \cdot kg^{-1}$)	Mean Acceleration ($m \cdot s^{-2}$)	Final velocity ($m \cdot s^{-1}$)	Impulse ($Bw \cdot s^{-1}$)
Non amputee (n=7)	Usual	**0.78 ± 0.09**	1.39 ± 0.24	11.94 ± 2.19	**7.63 ± 0.91**	3.09 ± 0.27	0.315 ± 0.028
	Unusual	**0.75 ± 0.09**	1.39 ± 0.26	11.36 ± 1.72	**7.39 ± 0.84**	3.05 ± 0.22	0.310 ± 0.022
Amputee (n=9)	UL in front	0.69±0.07	**1.12 ± 0.13**	9.59 ± 1.53	6.76 ± 0.65	2.81 ± 0.25	0.286 ± 0.026
	AL in front	0.68±0.10	**1.31 ± 0.18**	9.42 ± 2.52	6.67 ± 1.02	2.78 ± 0.37	0.283 ± 0.038

Table 4.3 - Mean and peak total (front + back) forces, mean accelerations final velocities and impulses at the end of the push-phase. All values are calculated in the horizontal direction and are reported as mean ± S.D. Highlighted gray indicates the value that results in the best performance between the two configurations. Statistically significant ($p<0.05$) differences between the 2 configurations within each group are highlighted in bold.

		Horizontal							
		Mean Force Back (BW)	Mean Force Front (BW)	Peak Force Back (BW)	Peak Force Front (BW)	Mean Power Back ($W \cdot kg^{-1}$)	Mean Power Front ($W \cdot kg^{-1}$)	Peak Power Back ($W \cdot kg^{-1}$)	Peak Power Front ($W \cdot kg^{-1}$)
Non amputees (n=7)	Usual	0.42 ± 0.11	0.62 ± 0.10	0.84 ± 0.22	1.02 ± 0.13	2.72 ± 1.10	11.30 ± 2.34	6.63 ± 2.75	26.51 ± 5.03
	Unusual	0.39 ± 0.07	0.62 ± 0.07	0.77 ± 0.12	1.00 ± 0.09	2.33 ± 0.54	11.02 ± 2.01	5.86 ± 1.40	25.62 ± 3.86
Amputees (n=9)	UL in front	**0.27 ± 0.13**	**0.60 ± 0.13**	**0.48 ± 0.21**	0.92 ± 0.18	**1.48 ± 1.04**	9.43 ± 2.22	**3.53 ± 2.38**	21.37 ± 5.40
	AL in front	**0.38 ± 0.13**	**0.52 ± 0.11**	**0.77 ± 0.25**	0.94 ± 0.13	**2.44 ± 1.40**	8.59 ± 2.41	**6.76 ± 3.16**	19.82 ± 6.56

Table 4.4 - Individual (front and back) leg forces and powers. All values are calculated in the horizontal direction and are reported as mean ± S.D. Highlighted gray indicates the value that results in the best performance between the two configurations. Statistically significant ($p<0.05$) differences between the 2 configurations within each group are highlighted in **bold**.

	Mean Resultant Force (BW)	Mean Push Angle (deg)	Horizontal acceleration ($m \cdot s^{-2}$)
Virtual non-amputee	**1.47 ± 0.13**	58.0 ± 1.9	**7.66 ± 0.94**
Virtual bilateral amputee	**1.16 ± 0.09**	59.1 ± 2.4	**5.84 ± 0.69**

Table 4.5 - Resultant forces, push angles and horizontal accelerations of virtual athletes. We calculated values for a virtual non-amputee by merging 2 UL and calculated values for a virtual bilateral amputee by merging 2 AL from the amputee group. Highlighted gray indicates the value that results in the best performance between the two conditions. Statistically significant ($p<0.05$) differences between the 2 conditions are highlighted in **bold**.

4.4.3.3 Virtual athletes

The virtual non-amputee sprinter calculations demonstrated much greater mean resultant forces (1.47 ± 0.13 vs. 1.16 ± 0.09 BW, p=0.0003, n=9) and mean horizontal accelerations (7.66 ± 0.94 vs. 5.84 ± 0.69 $m \cdot s^{-2}$, p=0.0001, n=9) compared to virtual bilateral amputee sprinters (table 5). However, there were no differences in mean push angles (figure 4.5).

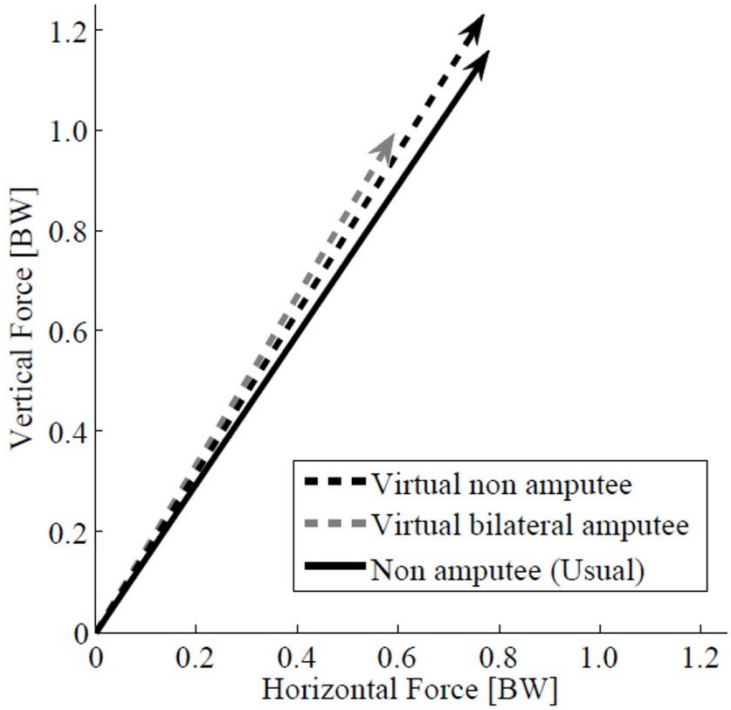

Figure 4.5 - Mean resultant force vectors (average values) for non-amputee (n=7), virtual non-amputee (n=9) and virtual bilateral amputee sprinters (n=9) . There were no differences between non–amputee and virtual non-amputee sprinters. Virtual non-amputee sprinters with 2 UL develop more force (p=0.0003) compared to virtual bilateral amputees with 2 AL.

4.5 Discussion

4.5.1 Non amputee

As expected, non-amputee sprinters had better horizontal acceleration, and therefore overall better starts, in their usual configuration. In their unusual configuration, all sprinters reported that they felt "uncomfortable" or "awkward". Despite this, total resultant force and push-angle were not statistically different compared to the usual configuration, indicating that it is the combination of both the resultant force and push angle that determines horizontal force and therefore acceleration. Although not surprising, we measured that leg preference has a quantifiable effect in sprint start performance. Single-leg values, however, were not different between configurations, suggesting that block configuration is not, or at least not only, based on the small differences in terms of power and/or force capability between right or left leg in non-amputee athletes, but most likely it's based on the brain's laterality. Like in hand preference, leg dominance seems to be the result of subtle differences in the brain hemispheres, rather than functional differences between right and left lower limb.

Our findings are parallel to previous studies (Mero 1988, Harland and Steele 1997) on non-amputee in the usual configuration. To the best of our knowledge, no previous studies measured force-time characteristics in sprinters adopting the unusual configuration. Morin et al. (2012) demonstrated that the magnitude of horizontal component of the ground reaction force in the acceleration was correlated with 100m performance, but the magnitude of the resultant force was not. Our data are in accordance with Morin et al. in that we find the slower start in the unusual configuration for non-amputees is the result of a sub-optimal combination of force magnitude and push-angle, rather than force deficiency alone.

4.5.2 Amputee

Sprinters with amputations had greater mean resultant forces in the usual configuration compared to the unusual one. When amputees put their unaffected leg on the front block, they developed 6% greater mean resultant forces. However, in contrast with our hypothesis, horizontal acceleration was not statistically different between the UL and AL in front configurations.

Unlike non-amputees, the combination of resultant force and push angle cancelled out any differences in horizontal acceleration between the UL and AL in front configurations: the greater mean resultant forces in the UL in front configuration were directed more upwards (+3%), causing a mere 1% improvement in horizontal acceleration, compared to the AL in front configuration.

Surprisingly, peak resultant and horizontal forces were greater in the AL in front compared to the UL in front configuration. As shown in Figure 2, non-amputee and amputee sprinters reach peak total force when they are pushing with both legs on the blocks: amputee sprinters, in particular, develop greater peak force with the back leg in the AL in front configuration (i.e. when they have the UL on the back block), therefore producing a greater peak total force than the UL in front configuration.

Apart from peak front force that was almost equal in the two configurations, the unaffected leg developed more force and power compared to the affected leg, when it was placed on the front block (UL in front) and on the back block (AL in front). In particular, when switching from UL in front to AL in front configuration, a 13% reduction of mean force in the front block due to the affected leg, was compensated by a 40% increment in the back block thanks to the unaffected leg.

4.5.3 Virtual athletes

In the Paralympics, athletes with a unilateral transtibial amputation (classified as T-44) compete in the same race as athletes with bilateral transtibial amputations (T-43). Although it has not yet been systematically quantified, it appeared that in the 2012 Paralympics, athletes with unilateral amputations had quicker starts than athletes with bilateral amputations, but athletes with bilateral amputations had higher speeds in the final part of the races. Our results provide some information on the debate if difference in terms of performance exist between unilateral and bilateral amputee sprinters and between non-amputee and amputee sprinters.

We used single-leg measurements from unilateral amputees to simulate the effect of having two unaffected legs or two affected legs with RSPs. Average values of mean resultant force, push angle and horizontal acceleration of virtual non-amputee sprinters showed no statistical difference with our non-amputee subjects using their usual configuration. Virtual bilateral amputee sprinters had worse start performance compared to virtual non-amputees: a 21% smaller resultant force and a 6% more vertical push-angle (although not statistically different), which resulted in a 23% slower horizontal acceleration. These virtual athletes support the impression that, among similar-level athletes (i.e. same overall times), bilateral amputees have slower starts than unilateral amputees, and unilateral amputees have slower starts than non-amputees.

4.5.4 Limitations

Although not statistically different, there was a 0.68s average difference in 100m PR times between non-amputees and amputees, a large time difference in sprint performance. Therefore, we did not statistically compare non-amputee and amputee groups. Future studies that match PR times from non-amputee and amputee subjects are desired to make statistical comparisons between groups.

We did not account for potential differences in body mass when we simulated virtual athletes. However, an RSP and socket have an approximate mass of 1.5 kg, while a biological lower leg has a mass of 4.9 kg for a 80kg male (Nolan 2008), a difference of only 3.4 kg. This difference is even reduced if we consider that all of our subjects had below-knee amputations, i.e. they maintained a portion of their biological lower leg. Therefore, we think that the effect of mass difference can be neglected, compared to the big % difference in acceleration. We plan to conduct further research of the sprint starts of bilateral amputees to further understand the effects of RSPs.

4.5.5 Future studies

Overall performance in a sprint race is influenced by many factors, including sprint starts and block configuration. Further investigation of the entire sprint race is necessary to understand how RSPs compare to biological limbs.

4.6 References

Bezodis NE, Salo AI, Trewartha G. (2008) Understanding elite sprint start performance through an analysis of joint kinematics. *ISBS Conference*

Buckley JG. (2000) Biomechanical adaptations of transtibial amputee sprinting in athletes using dedicated prostheses. *Clin Biomech* 15(5):352-8

di Prampero PE, Fusi S, Sepulcri L, Morin JB, Belli A, Antonutto G.(2005) Sprint running: a new energetic approach. *Journal of experimental biology*, *208*(14), 2809-2816

Eikenberry A, McAuliffe J, Welsh TN, Zerpa C, McPherson M, Newhouse I. (2008) Starting with the "right" foot minimizes sprint start time. *Acta psychologica*, *127*(2), 495-500

Fortier S, Basset FA, Mbourou GA, Favérial J, Teasdale N. (2005) Starting block performance in sprinters - a statistical method for identifying discriminative parameters of the performance and an analysis of the effect of providing feedback over a 6-week period. *J Sport Sci Med* 4:134-143

Gutiérrez-Dávilla M, Dapena J, Campos J. (2006) The effect of muscular pre-tensing on the sprint start. *J Appl Biomech* 22(3):194-201

Grabowski A M, McGowan CP, McDermott WJ, Beale MT, Kram R, Herr HM. (2010) Running-specific prostheses limit ground-force during sprinting. *Biology Letters*, *6*(2), 201-204

Harland MJ, Steele, JR. Biomechanics of the sprint start.(1997) *Sports Medicine*, *23*(1), 11-20

Hautier CA, Wouassi D, Arsac LM, Bitanga E, Thiriet P, Lacour JR. (1994) Relationships between postcompetition blood lactate concentration and average running velocity over 100-m and 200-m races. *European journal of applied physiology and occupational physiology*, *68*(6), 508-513

IAAF Competition Rules 2012-2013. www.iaaf.org

Mero A. (1988) Force-time Characteristics and Running Velocity of Male Sprinters During the Acceleration Phase of Sprinting. *Res Q Exerc Sport* 59(2):94-98

Morin JB, Bourdin M, Edouard P, Peyrot N, Samozino P, Lacour JR. (2012) Mechanical determinants of 100-m sprint running performance. *European journal of applied physiology*, 112(11):3921-3930

Newton RU, Gerber A, Nimphius S, Shim JK, Doan BK, Robertson M, Pearson DR, Craig BW, Häkkinen K, Kraemer WJ. (2006) Determination of functional strength imbalance of the lower extremities. *J Strength Cond Res* 20(4):971-7

Nolan L. (2008) Carbon fibre prostheses and running in amputees: A review. *Foot and ankle surgery*, *14*(3), 125-129

Multimedia

"Women's T44(BK) 100m Bejing 2008 Final" 14 September 2008. Accessed on 7 November 2012. Online video clip. Youtube. <http://www.youtube.com/watch?v=estn6ST7EFY>

"Women's 200m T44 - Beijing 2008 Paralympic Games" 12 March 2012. Accessed on 7 November 2012. Online video clip. Youtube. <http://www.youtube.com/watch?v=Xqytj5PP0dw>

"Men's 100 m T44 - Beijing 2008 Paralympic Games " 8 March 2012. Accessed on 7 November 2012. Online video clip. YouTube. <http://www.youtube.com/watch?v=UDDhZx54Jy4>

"Men's 200m T44 - Beijing 2008 Paralympic Games" 25 May 2012. Accessed on 7 November 2012. Online video clip. Youtube.<http://www.youtube.com/watch?v=0wK2MjLM69c>

"Athletics - Women's 100m - T44 Final - London 2012 Paralympic Games " 4 September 2012. Accessed on 7 November 2012. Online video clip. Youtube. <http://www.youtube.com/watch?v=2_vPxntIHI8>

"Athletics - Women's 200m - T44 Final - London 2012 Paralympic Games " 7 September 2012. Accessed on 7 November 2012. Online video clip. Youtube. <http://www.youtube.com/watch?v=mbLpLxKmupY>

"Athletics - Men's 100m - T44 Final - London 2012 Paralympic Games " 7 September 2012. Accessed on 7 November 2012. Online video clip. Youtube. <http://www.youtube.com/watch?v=mcdUsMULNzo>

"Athletics - Men's 200m - T44 Final - London 2012 Paralympic Games" 2 September 2012. Accessed on 7 November 2012. Online video clip. Youtube. <http://www.youtube.com/watch?v=A9Wlp1sTnoY>

5. Part IIb: Maximum speed curve running biomechanics of sprinters with and without unilateral leg amputations

5.1 Introduction

Previous research has quantified how curve radius influences maximum running speed on unbanked (flat) curves, and concluded that the smaller the curve radius, the slower the speed (Greene, 1985; Usherwood and Wilson, 2005; Chang and Kram, 2007; Luo and Stefanyshyn, 2012; Ferro and Floria, 2013). For example, Chang and Kram showed that the maximum speed when running around a 6m radius curve was 26% slower than straight running maximum speed. The effects of curve running and speed could have important consequences for competitive athletics.

Track and field athletes participating in 200 m and 400 m events must negotiate one or two curves, respectively, on an outdoor track. On an 8 lane standard 400 m outdoor track, the inner lane curve radius is 36.50 m, while the outer lane curve radius is 45.04 m (IAAF Track and Field Facilities Manual 2008). In the 200 m event, Greene (1985) calculated a 0.123 s advantage for an elite-level sprinter (average speed: 10 $m \cdot s^{-1}$) running in lane 8 compared to running in lane 1. However, Morton (1997) found no statistical correlation between lane assignment in international track and field competitions and 200 m or 400 m running times. This discrepancy may be due to the seeding rules employed in major track and field competitions (World Championships, Olympic Games etc.), where runners who have performed best in previous rounds are assigned the central lanes. In addition, psychological factors may mitigate the potential mechanical disadvantage of being assigned to an inner lane (i.e. an athlete in the first lane can see all the other competitors and therefore may be motivated to run faster) (Morton, 1997). The

effects of curve radius, and therefore lane assignment, on sprint performances are profound on indoor tracks, where the lane 1 curve radius can be as small as 15 m (the recommended radius being 17.2 m, IAAF Track and Field Facilities Manual 2008). In fact, in 2005 the International Association of Athletics Federations (IAAF) abandoned indoor 200 m races because the athletes assigned to outer lanes showed a clear advantage over those assigned to inner lanes.

Greene (1985) proposed that curve running speed is limited by the maximum resultant force that an athlete can apply to the ground. A person running on a curve must apply a centripetal force to change his/her direction, while simultaneously applying a vertical force to counteract gravity. The vector sum of centripetal and vertical forces is the resultant force (see chapter 1.4.4). According to Greene, there is a physiological limit on the maximum resultant leg force that can be exerted by an individual. If Greene is correct, because running along a smaller curve radius requires a greater centripetal force, the maximum vertical force that can be applied must be lower compared to running along a larger curve radius. A smaller vertical force necessitates a longer ground contact time in order to support body weight. Because the distance traveled during foot contact remains the same during sprinting (McMahon and Greene, 1979), a prolonged contact time would result in a slower speed during curve running. Chang and Kram (2007), however, showed that subjects sprinting on curves generated significantly smaller resultant forces compared to straight sprinting. Their results indicate that curve running maximum speed is not limited by a physiological upper limit to resultant leg force. Further, Chang and Kram argued that because the inside leg generates smaller forces compared to the outside leg, it is the inside leg mechanics that limit curve running maximum speed.

Because the legs of non-amputees are essentially symmetric, a similar maximal curve-running speed would be expected in clockwise or counterclockwise directions.

However, given that all track events are customarily run in the counterclockwise direction, athletes may run faster in the counterclockwise direction because they are much more familiar with this orientation. In contrast, the legs of sprinters with unilateral leg amputations are not symmetric, which may have implications for curve running performance.

To our knowledge, no previous study has measured the biomechanics of curve running in athletes with leg amputations. These sprinters use running-specific prostheses (RSPs), which are typically J-shaped carbon-fiber passive springs intended to replicate the sagittal plane action of a biological ankle. During the first half of the stance phase of running, an athlete loads the RSP and stores elastic energy.. Then, during the second half of the stance phase, the RSP returns the elastic energy. Elastic energy plays a substantial role in moderate speed running (Ker et al. 1987, Farley et al. 1993). However, in athletes with unilateral amputations, the compliance of an RSP and the absence of mechanical power production by an RSP reduce the ability of the affected leg to generate peak vertical ground reaction forces. At sprinting speeds, athletes with a unilateral transtibial amputation generate 16% smaller peak vertical forces with their affected leg compared to their unaffected leg (Grabowski et al. 2010). In addition, McGowan et al. (2012) showed that non-amputee sprinters increase their leg stiffness across running speeds up to top sprinting speeds. However, they found that sprinters with unilateral transtibial amputations can maintain their unaffected leg stiffness across speeds, but exhibit a 17% decrease in their affected leg stiffness across speeds. Thus, the mechanical behavior of affected legs with RSPs is quite different than the mechanical behavior of biological legs, particularly at sprinting speeds (>6 m $\cdot$ s^{-1}).

RSPs primarily store and return elastic energy in the sagittal plane, mimicking the Achilles tendon's action to plantar-flex the ankle. But, due to their design, RSPs are torsionally stiff and resist inversion/eversion. Although the non-sagittal

mechanics of RSPs are not well understood, RSPs may impede the optimal inversion and eversion necessary for curve running (Greene 1987, Luo and Stefanyshyn 2012).

Figure 5.1 – Men's 200m T43-T44 final in London 2012 Paralympic Games. Sprinters in lanes 6 and 9 have the RSP on the left side, sprinters in lanes 3 and 8 have the RSP on the right side, all other athletes have bilateral amputations.

5.2 Aims of the study

Our first objective was to compare curve running performance between non-amputee sprinters and sprinters with unilateral transtibial amputations. We hypothesized that athletes without and with unilateral transtibial amputations would be slower during maximal speed curve running compared to maximal speed straight running. Given that the inside leg is thought to limit curve running speed, our second objective was to determine if the curve running performances of athletes with left or right unilateral leg amputations would be differently affected in clockwise and counterclockwise curves. We hypothesized that sprinters with a unilateral leg amputation would be slower in curves with their affected leg on the inside of the curve, compared to curves with their affected leg on the outside of the curve.

5.3 Materials and methods

5.3.1 Subjects

A total of 14 subjects participated: 6 (5M/1F) non-amputee sprinters, 6 (5M/1F) sprinters with a right leg transtibial amputation, and 2 (1M/1F) sprinters with a left leg transtibial amputation. All subjects gave their informed consent before participating in this study as per the University of Colorado Institutional Review Board.

5.3.2 Experimental design

Each subject performed a total of six 40 m sprints on a standard synthetic track surface, wearing their own spiked shoes. The curve of the track was not banked and had a radius of 17.2 m. Each subject performed two sprints in a straight direction (S), two on a clockwise (CW) curve and two on a counterclockwise (CCW) curve. We measured the 20 m and 40 m marks with a measuring wheel (Stanley MW40) and marked the start, 20 m and 40 m marks on the ground with tape. During each trial, subjects ran as fast as possible from a standing start. For the curve running trials, we asked the subjects to run as close as possible to the inner line of the curve without touching it. Between each trial, 8 minutes of rest were enforced. For each subject, we selected a random sequence of S, CW and CCW directions for the first set of three sprints. Then, we reversed the sequence for the second set of three sprints in order to control for any potential effects of fatigue. For example, one possible full sequence was: CW-S-CCW-CCW-S-CW.

We used a high-speed video camera (Casio EX-FH20, Casio Computer Co., LTD, Japan) with a frame-rate of 210 fps to record each subject during each trial. For the straight trials, we placed the camera on a tripod perpendicular to the 30 m

mark, approximately 50 m away from the track, in order to minimize parallax error (Fig. 1). For the curve trials, we placed the camera on a tripod at the center of the curve (Fig.1) and manually panned the camera to keep the subject in the field of view throughout the curve running trials. We used Kinovea 0.8.15 video-analysis software (Joan Charmant & Contrib. http://www.kinovea.org) to analyze each trial. We measured the time interval between the 20 m and 40 m marks, and calculated mean running velocity. We identified the beginning and end of the time interval as the frames when the vertical projection of chest of the subject crossed the marks on the ground. For each leg, we measured ground contact time, leg swing time (subsequent to the leg's foot-ground contact time), aerial time (subsequent to the leg's contact time) and step time (the time from foot-ground contact to contralateral foot-ground contact, see Figure 2). We then multiplied step time by running velocity to obtain step length.

We calculated step time asymmetry as:

$$Asymmetry = ((Right - Left)/(Right + Left)) \cdot 100 \quad (5.1)$$

positive values indicate a longer step time with the right leg, negative values indicate a longer step time with the left leg, while 0% indicates perfect symmetry. We performed the same step time asymmetry calculation for the sprinters with amputations, using unaffected and affected legs instead of right and left legs, respectively.

	Subject	Sex (M/F)	Age (years)	Height (m)	Mass (kg)	100m PR (s)	RSP Model
Non-amputees	1	M	18	1.73	66.7	11.58	-
	2	M	44	1.75	75.1	11.8	-
	3	M	33	1.75	65.8	12.22	-
	4	M	22	1.8	95	12.30	-
	5	M	19	1.82	96	12.96	-
	6	F	24	1.65	74.1	14.75	-
Average ± S.D.			26.7 ± 10.0	1.75 ± 0.06	78.8 ± 13.5	12.60 ± 1.15	
Right Leg Amputation	1	M	29	1.83	73.9	11.90	Ottobock Sprinter
	2	M	33	1.91	112.3	12.14	Ottobock Sprinter
	3	M	24	1.75	74.5	12.40	Ossur Cheetah
	4	M	28	1.88	79.6	12.60	Ossur Flexfoot Sprint
	5	M	28	1.7	60.7	26.33 (200m)	Ossur Cheetah
	6	F	21	1.7	59	15.63	Ottobock Sprinter
Average ± S.D.			27.2 ± 4.2	1.80 ± 0.09	76.7 ± 19.3	12.98 ± 1.37	
Left Leg Amputation	1	F	27	1.7	64.2	13.61	Ottobock Sprinter
	2	M	18	1.78	92.2	14.50	Ossur Cheetah
Average ± S.D.			22.5 ± 6.4	1.74 ± 0.06	78.2 ± 19.8	14.06 ± 0.63	

Table 5.1 - Subject characteristics. Demographic and anthropometric variables and 100m personal records (PR) of non-amputee and amputee subjects. Each amputee subject's running specific prosthesis (RSP) model is reported. Average values ± standard deviations are reported for all groups.

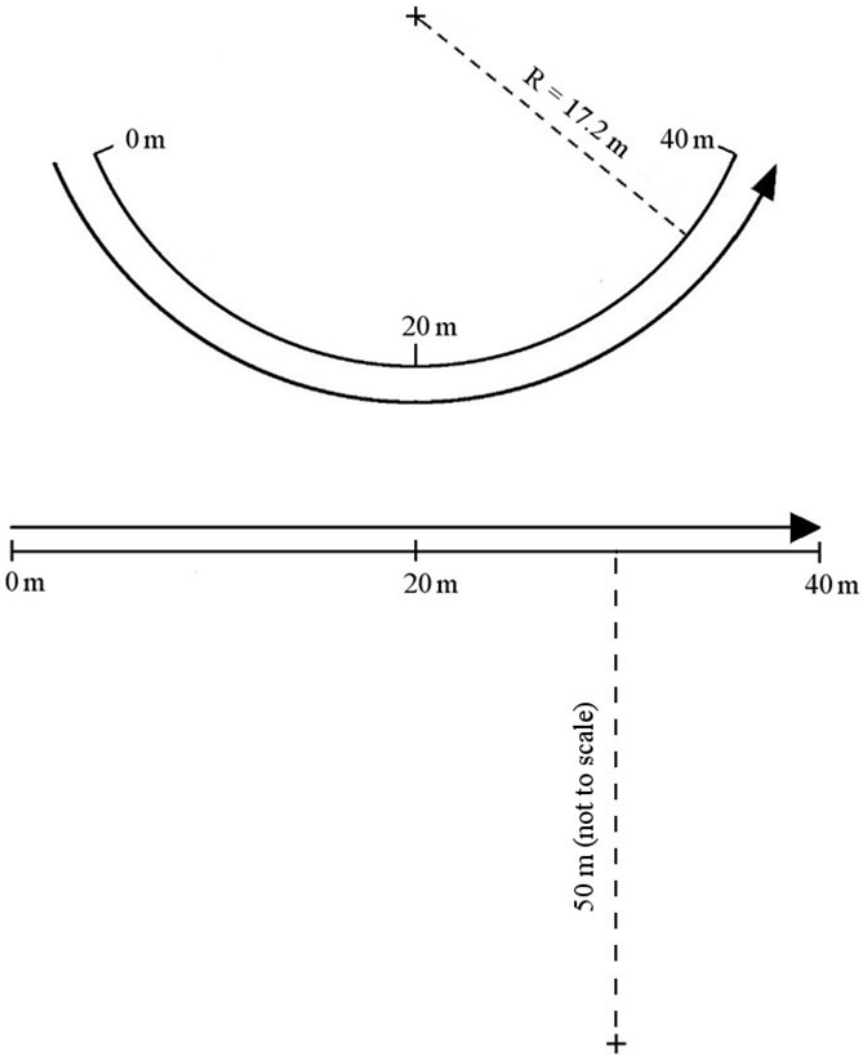

Figure 5.2 – Top view of the experimental set up. Counterclockwise curve (upper panel) and straight (lower panel). For the clockwise curve, subjects started from the 40m mark and ran to the 0m mark. All measurements were performed for the last 20m of each run. The cross + indicates camera placement.

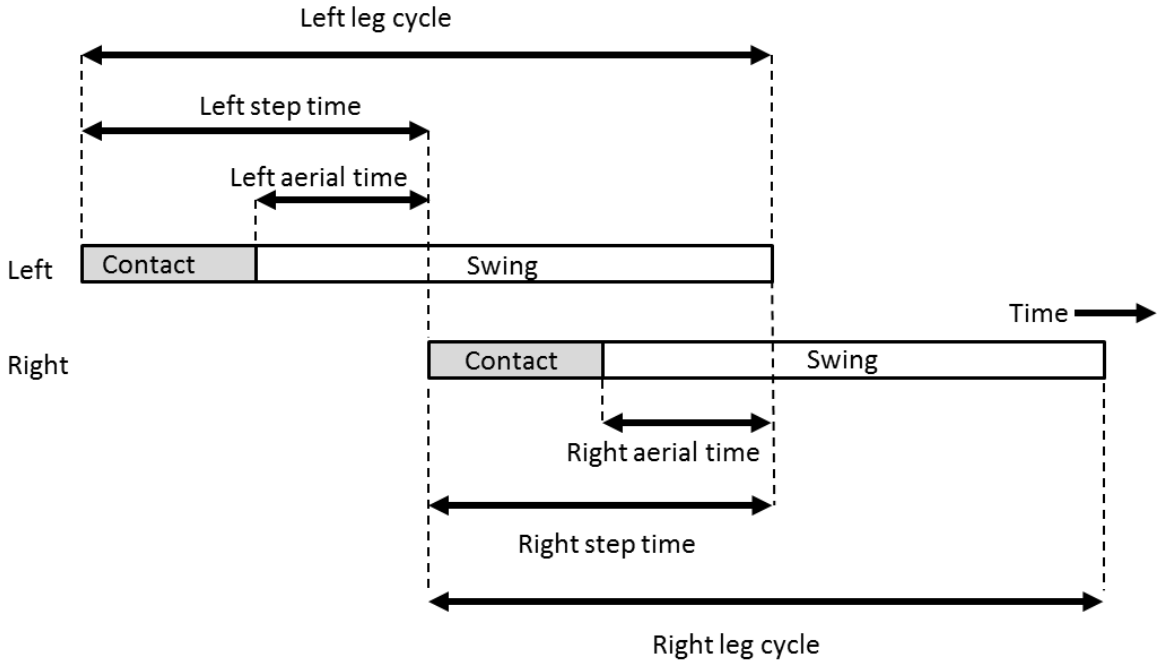

Figure 5.3. Schematic view of the measured gait parameters. Step time is defined as the time from foot contact to contralateral foot contact, aerial time is defined as the time from the end of the contact phase to the contralateral foot contact, leg cycle is defined as the sum of contact and swing times.

5.3.3 Statistical analysis

We checked the normality of the samples with the Shapiro-Wilk test and then used a paired samples t-test to assess the differences between straight, counterclockwise and clockwise running in non-amputees and sprinters with right leg amputations. We did not perform statistical tests on the sprinters with left leg amputations given the small sample size of this group (n=2).

We subsequently combined sprinters with right and left leg amputations into a single group and distinguished the curves where runners had their affected leg on the outside versus on the inside of the curve. We used a paired samples t-test to assess differences between these conditions. A p value of less than or equal to 0.05 was accepted as significant.

5.4 Results

We primarily present data for two groups: the non-amputee sprinters and all of the sprinters with amputations. For non-amputee sprinters, we distinguish between straight, clockwise and counterclockwise curves. For sprinters with amputations, we distinguish between straight, curves with the affected leg on the outside and curves with the affected leg on the inside. To elucidate how a right versus left leg amputation affects performance, in the tables we also present data for athletes with right and left leg amputations. All values are reported as average ± standard deviation.

5.4.1 Average speed

Non-amputee sprinters ran the last 20 m of the straight running trials faster (8.05 ± 0.65 $m \cdot s^{-1}$) compared to the counterclockwise (7.39 ± 0.49 $m \cdot s^{-1}$) and clockwise (7.25 ± 0.45 $m \cdot s^{-1}$) curves (p=0.002 and p=0.001 respectively). There were no statistical differences in speed between the counterclockwise and clockwise directions.

All of the sprinters with leg amputations ran faster during the straight trials (7.82 ± 0.63 $m \cdot s^{-1}$), compared to curve running with their affected leg on the outside (7.43 ± 0.56 $m \cdot s^{-1}$) and curve running with their affected leg on the inside (7.05 ± 0.51 $m \cdot s^{-1}$) (p=0.001 for both comparisons). Athletes ran faster during curve running with their affected leg on the outside compared to their affected leg on the inside (p=0.029). Only one sprinter (with a left leg amputation) ran slower, by only 0.9%, during curve running with her affected leg on the outside versus the inside.

	Velocity ($m \cdot s^{-1}$)		
	Straight	Counterclockwise	Clockwise
Non-amputees (n=6)	8.05 ± 0.65*	7.39 ± 0.49	7.25 ± 0.45
Right Leg Amputation (n=6)	7.99 ± 0.60*	**7.58 ± 0.56**	**7.12 ± 0.53**
Left Leg Amputation (n=2)	7.30 ± 0.50	6.86 ± 0.58	6.97 ± 0.34
	Straight	RSP outside	RSP inside
All amputees (n=8)	7.82 ± 0.63*	**7.43 ± 0.57**	**7.05 ± 0.51**

Table 5.2 - Average velocity for straight, counterclockwise curve, and clockwise curve running trials (radius = 17.2m). Bold values indicate a statistical difference between the counterclockwise and clockwise directions or between the affected leg on the outside and affected leg in the inside values. * indicate a statistical difference between straight and curve running trials. For the sprinters with left leg amputations (n=2), no statistical tests were performed. Non-amputees and sprinters with right leg amputations were all slower during curve running compared to straight running. The sprinters with right leg amputations had significantly different running speeds in the counterclockwise vs. clockwise directions (p=0.035). All athletes with amputations ran slower when their affected leg was on the inside of the curve (p=0.029).

5.4.2 Contact time

Non-amputees had equivalent right and left leg contact times during straight running (Table 5.3). During curve running, the inside leg had longer contact times than the outside leg in the counterclockwise curve (0.140 ± 0.013 s vs. 0.130 ± 0.015 s, respectively; $p<0.001$) and in the clockwise curve (0.141 ± 0.013 s vs. 0.131 ± 0.015 s, respectively; $p=0.004$). In addition, during curve running, both legs' contact times were significantly longer compared to straight running.

All of the sprinters with leg amputations had longer contact times with their affected leg compared to their unaffected leg in the straight running trials (0.126 ± 0.013 s vs. 0.111 ± 0.011 s, respectively; $p<0.001$) and in curve running with their affected leg on the inside of the curve (0.144 ± 0.010 s vs. 0.127 ± 0.011 s, respectively; $p<0.001$). There were no statistical differences in contact times between affected and unaffected legs in curves with the affected leg on the outside of the curve. The affected leg contact times were longer during both curves compared to straight running trials ($p<0.001$ for curves with the affected leg on the inside and $p=0.011$ for curves with the affected leg on the outside). The unaffected leg contact times were longer in both curves compared to straight running ($p=0.001$ for curves with the affected leg on the inside and $p<0.001$ for curves with the affected leg on the outside). Overall, during curve running, both legs' contact times were longer compared to straight running, but the effect was more pronounced for the inside leg.

	Contact time (s)					
	Straight		Counterclockwise		Clockwise	
	Left	Right	Left	Right	Left	Right
Non-amputees	0.117 ± 0.012	0.116 ± 0.011	0.140 ± 0.013	0.130 ± 0.015	0.131 ± 0.015	0.141 ± 0.013
Right Leg Amputation	**0.110 ± 0.004**	**0.125 ± 0.010**	0.133 ± 0.007	0.132 ± 0.007	**0.127 ± 0.007**	**0.143 ± 0.007**
Left Leg Amputation	0.128 ± 0.025	0.117 ± 0.025	0.148 ± 0.022	0.127 ± 0.025	0.139 ± 0.029	0.133 ± 0.010
	Straight		AL outside		AL inside	
	AL	UL	AL	UL	AL	UL
All amputees	**0.126 ± 0.013**	**0.111 ± 0.011**	0.134 ± 0.013	0.133 ± 0.007	**0.144 ± 0.010**	**0.127 ± 0.011**

Table 5.3 - Contact time. Bold values indicate a statistical difference between left and right legs and between affected and unaffected legs in the same condition (straight, counterclockwise or clockwise). Non-amputees had no difference in contact times between right and left legs in all conditions. In sprinters with right leg amputations, contact times were longer for the right leg (AL) in the straight ($p=0.006$) and clockwise ($p=0.002$) direction compared to the left leg (UL). There were no differences in contact times between right (AL) and left (UL) legs in the counterclockwise direction. All sprinters with amputations had longer contact times in their affected leg compared to their unaffected leg during straight running ($p=0.001$) and during curve running with the affected leg on the inside ($p<0.001$).

.4.3 Aerial time

Non-amputees had equivalent left and right leg aerial times in all conditions (Table 5.4). During curve running, both legs' aerial times were shorter compared to straight running. Left leg aerial times were shorter in counterclockwise curves compared to straight running (0.106 ± 0.013 s vs. 0.118 ± 0.013 s, respectively; p=0.018) and in clockwise curves compared to straight running (0.105 ± 0.010 s vs. 0.118 ± 0.013 s, respectively; p=0.001). Right leg aerial times were shorter in counterclockwise curves compared to straight running (0.101 ± 0.014 s vs. 0.114 ± 0.007 s; p=0.006) and in clockwise curves compared to straight running (0.104 ± 0.010 s vs. 0.114 ± 0.007 s, respectively; p=0.029).

All of the sprinters with amputations had longer aerial times with their affected leg compared to their unaffected leg in the straight running trials (0.127 ± 0.013 s vs. 0.113 ± 0.017 s, respectively; p=0.006). During curve running trials, there were no statistical differences in aerial times between affected and unaffected legs. In curves with the affected leg on the outside aerial times were shorter compared to straight running trials for the affected leg (0.110 ± 0.014 s vs. 0.127 ± 0.013 s, respectively; p=0.002) and for the unaffected leg (0.103 ± 0.015 s vs. 0.113 ± 0.017 s, respectively; p<0.001). There were no statistical differences in aerial times in curves with the affected leg on the inside compared to straight running trials.

	Aerial time (s)					
	Straight		Counterclockwise		Clockwise	
	Left	Right	Left	Right	Left	Right
Non-amputees	0.118 ± 0.013	0.114 ± 0.007	0.106 ± 0.013	0.101 ± 0.014	0.105 ± 0.010	0.104 ± 0.010
Right Leg Amputation	**0.117 ± 0.012**	**0.131 ± 0.010**	0.107 ± 0.012	0.113 ± 0.008	0.115 ± 0.008	0.124 ± 0.007
Left Leg Amputation	0.115 ± 0.018	0.101 ± 0.028	0.119 ± 0.013	0.098 ± 0.016	0.100 ± 0.028	0.094 ± 0.024
	Straight		AL outside		AL inside	
	AL	UL	AL	UL	AL	UL
All amputees	**0.127 ± 0.013**	**0.113 ± 0.017**	0.110 ± 0.014	0.103 ± 0.015	0.123 ± 0.010	0.111 ± 0.013

Table 5.4 - Aerial time. Bold values indicate a statistical difference between left and right legs and between affected and unaffected legs in the same condition (straight, counterclockwise or clockwise).

5.4.3 Step time

Non-amputees had equivalent left and right leg step times within all conditions (Table 5.5). During curve running, the inside leg step times were significantly longer compared to the same leg's contact times during straight running. Left leg step times were longer in the counterclockwise direction compared to straight running (0.246 ± 0.019 s vs. 0.235 ± 0.015 s, respectively; p=0.031). Right leg step times were longer in the clockwise direction compared to straight running (0.245 ± 0.011 s vs. 0.230 ± 0.008 s, respectively; p=0.008).

All of the sprinters with amputations had longer affected leg step times compared to unaffected leg step times in the straight running trials (0.253 ± 0.012 s vs. 0.224 ± 0.013 s, respectively; p<0.001) and in curve running with their affected leg on the inside of the curve (0.267 ± 0.014 s vs. 0.238 ± 0.011 s, respectively; p<0.001). There were no statistical differences in step times between affected and unaffected legs in curves with the affected leg on the outside of the curve. The affected leg step times were longer in curves with the affected leg on the inside compared to straight running trials (p=0.015). The unaffected leg step times were longer in both curves compared to straight running (p=0.006 for curves with the affected leg on the inside and p=0.005 for curves with the affected leg on the outside).

	Step time (s)					
	Straight		Counterclockwise		Clockwise	
	Left	Right	Left	Right	Left	Right
Non-amputees	0.235 ± 0.015	0.230 ± 0.008	0.246 ± 0.019	0.231 ± 0.009	0.236 ± 0.013	0.245 ± 0.011
Right Leg Amputation	**0.226± 0.014**	**0.256± 0.012**	0.240 ± 0.012	0.245 ± 0.012	**0.243± 0.008**	**0.267± 0.016**
Left Leg Amputation	0.242 ± 0.007	0.218 ± 0.003	0.266 ± 0.008	0.224 ± 0.009	0.240 ± 0.001	0.227 ± 0.014
	Straight		AL outside		AL inside	
	AL	UL	AL	UL	AL	UL
All amputees	**0.253± 0.012**	**0.224± 0.013**	0.244 ± 0.11	0.236 ± 0.013	**0.267± 0.014**	**0.238± 0.011**

Table 5.5 - Step time. Bold values indicate a statistical difference between left and right legs and between affected and unaffected legs in the same condition (straight, counterclockwise or clockwise).

5.4.5 Step length

Non-amputees had equivalent left and right leg step lengths in all conditions (Table 5.6). During curve running, non-amputees took shorter steps with their outside leg compared to the same leg in straight running trials. The right leg step lengths were shorter in counterclockwise curves compared to straight running trials (1.71 ± 0.12 m vs. 1.85 ± 0.13 m, respectively; $p<0.001$). The left leg step lengths were shorter in clockwise curves compared to straight running trials (1.71 ± 0.11 m vs. 1.89 ± 0.11 m, respectively; $p=0.002$).

All of the sprinters with amputations took longer steps with their affected leg compared to their unaffected leg in straight running trials (1.98 ± 0.21 m vs. 1.76 ± 0.21 m, respectively; $p<0.001$) and in curves with the affected leg on the inside (1.88 ± 0.10 m vs. 1.68 ± 0.13 m, respectively; $p=0.001$). There were no statistical differences in step length between affected and unaffected legs in curves with the affected leg on the outside. The affected leg step lengths were shorter in curves with the affected leg on the outside compared to the same leg's step length in straight running trials (1.81 ± 0.11 m vs. 1.98 ± 0.21 m, respectively; $p=0.004$). There were no statistical differences in the affected leg step length between curves with the affected leg on the inside and straight running trials. There were no statistical differences in the unaffected leg step length between curves and straight running trials.

Figure 5.4 - Two subsequent steps of a sprinter with a right leg amputation during a counterclockwise curve (upper panel) and during a clockwise curve (lower panel). In both configurations, the step length is longer with the inside leg.

	Step length (m)					
	Straight		Counterclockwise		Clockwise	
	Left	Right	Left	Right	Left	Right
Non-amputees	1.89 ± 0.11	1.85 ± 0.13	1.81 ± 0.10	1.71 ± 0.12	1.71 ± 0.11	1.77 ± 0.06
Right Leg Amputation	**1.81 ± 0.21**	**2.05 ± 0.20**	1.82 ± 0.17	1.85 ± 0.08	**1.73 ± 0.11**	**1.90 ± 0.10**
Left Leg Amputation	1.76 ± 0.07	1.59 ± 0.13	1.82 ± 0.10	1.54 ± 0.07	1.67 ± 0.08	1.58 ± 0.17
	Straight		AL outside		AL inside	
	AL	UL	AL	UL	AL	UL
All amputees	**1.98 ± 0.21**	**1.76 ± 0.21**	1.81 ± 0.11	1.76 ± 0.19	**1.88 ± 0.10**	**1.68 ± 0.13**

Table 5.6 - Step length. Bold values indicate a statistical difference between left and right legs and between affected and unaffected legs in the same condition (straight, counterclockwise or clockwise).

5.4.6 Leg Swing time

Non-amputees had equivalent left and right leg swing times during the straight running trials (Table 5.7). During counterclockwise curve running, inside (left) leg swing times were shorter compared to outside (right) leg swing times (0.336 ± 0.020 s vs. 0.347 ± 0.022 s, respectively; p=0.040). During clockwise curve running, inside (right) leg swing times were again shorter compared to outside (left) leg swing times (0.340 ± 0.014 s vs. 0.350 ± 0.015 s, respectively; p=0.004). Only the left (inside) leg swing times were significantly shorter in the counterclockwise direction compared to straight running trials (p=0.011).

All of the sprinters with leg amputations had shorter affected leg swing times compared to unaffected leg swing times during straight running trials (0.351 ± 0.022 s vs. 0.366 ± 0.023 s, respectively; p<0.001) and in curves with the affected leg on the inside (0.361 ± 0.021 s vs. 0.378 ± 0.016 s, respectively; p<0.001). There were no statistical differences between affected and unaffected leg swing times during curves with the affected leg on the outside. The unaffected leg swing times were shorter in curves with the affected leg on the outside compared to straight running trials (p=0.006) while they were longer in curves with the affected leg on the inside compared to straight running trials (p=0.035). We found no differences between the affected leg swing times between curves and straight running trials. In other words, sprinters with leg amputations were able to modify the leg swing times of their unaffected leg (reducing it when it was on the inside of the curve and increasing it when it was on the outside), but not the leg swing times of their affected leg.

	Swing time (s)					
	Straight		Counterclockwise		Clockwise	
	Left	Right	Left	Right	Left	Right
Non-amputees	0.348 ± 0.018	0.349 ± 0.017	**0.336 ± 0.020**	**0.347 ± 0.022**	**0.350 ± 0.015**	**0.340 ± 0.014**
Right Leg Amputation	**0.373 ± 0.020**	**0.358 ± 0.020**	0.352 ± 0.016	0.353 ± 0.018	**0.383 ± 0.015**	**0.367 ± 0.021**
Left Leg Amputation	0.332 ± 0.021	0.343 ± 0.021	0.343 ± 0.004	0.364 ± 0.008	0.327 ± 0.042	0.333 ± 0.024
	Straight		AL outside		AL inside	
	AL	UL	AL	UL	AL	UL
All amputees	**0.351 ± 0.022**	**0.366 ± 0.023**	0.347 ± 0.025	0.347 ± 0.019	**0.361 ± 0.021**	**0.378 ± 0.016**

Table 5.7 - Leg swing time. Bold values indicate a statistical difference between left and right legs and between affected (AL) and unaffected legs (UL) in the same condition (straight, counterclockwise or clockwise). Non-amputees had faster leg swing times for their left leg during counterclockwise curves ($p=0.040$) and had slower leg swing times in their left leg during clockwise curves ($p=0.004$). Sprinters with right leg amputations had faster leg swing times in their affected leg (AL) compared to their unaffected leg (UL) during straight running ($p=0.0004$) and during clockwise ($p<0.001$) running. All sprinters with amputations had faster leg swing times in their affected leg compared to unaffected leg during straight running ($p<0.001$) and curve running with the affected leg on the inside ($p<0.001$).

5.4.3 Step asymmetry

Non-amputees had nearly symmetric step times in straight running trials (-1.0 ± 2.0 %, see Table 5.8). During counterclockwise curve running, step asymmetry was -3.0 ± 3.3 % (longer step times with the left leg); during clockwise curve running, step asymmetry was 1.8 ± 2.1 % (longer step times with the right leg). During both curves, the asymmetry was not statistically different compared to straight running trials. Between counterclockwise and clockwise curves the difference (4.9 ± 4.1 %) was statistically significant (p=0.033).

The sprinters with leg amputations had an average step time asymmetry of 6.0 ± 2.7 % (longer step times with the affected leg). There were no statistical differences in step time asymmetry for curves with the affected leg on the inside (5.7 ± 3.0 %) compared to straight running trials. The asymmetry was reduced in curves with the affected leg on the outside (1.5 ± 3.0 %) compared to straight running trials (p=0.001). Step time asymmetries between curves with the affected leg on the outside and curves with the affected leg on the inside were statistically different (p=0.009). In other words, we found that sprinters had more symmetrical step times in curves with their affected leg on the outside of the curve, but greater asymmetry in curves with their affected leg on the inside of the curve.

	Leg asymmetry (%)		
	Straight	Counterclockwise	Clockwise
Non-amputees	-1.0 ± 2.0	**-3.0 ± 3.3**	**1.8 ± 2.1**
Right Leg Amputation	6.2 ± 3.0	**1.1 ± 3.1**	**4.8 ± 2.8**
Left Leg Amputation	-5.3 ± 2.1	-8.5 ± 0.4	-2.4 ± 3.2
	Straight	AL outside	AL inside
All amputees	6.0 ± 2.7	**1.5 ± 3.0**	**5.7 ± 3.0**

Table 5.8. Average ± S.D. step time symmetry. Step time symmetry is calculated as ((Right-Left)/(Right+Left))*100 for non-amputees and as (AL-UL)/(AL+UL)*100 for all amputees. A value of 0% would indicate perfect symmetry, positive values indicate that right leg (AL for all amputees) had longer step times, negative values indicates that left leg (UL) had longer step times. Bold values indicate a statistical difference between the counterclockwise and clockwise directions or between the affected leg on the outside and affected leg in the inside values.

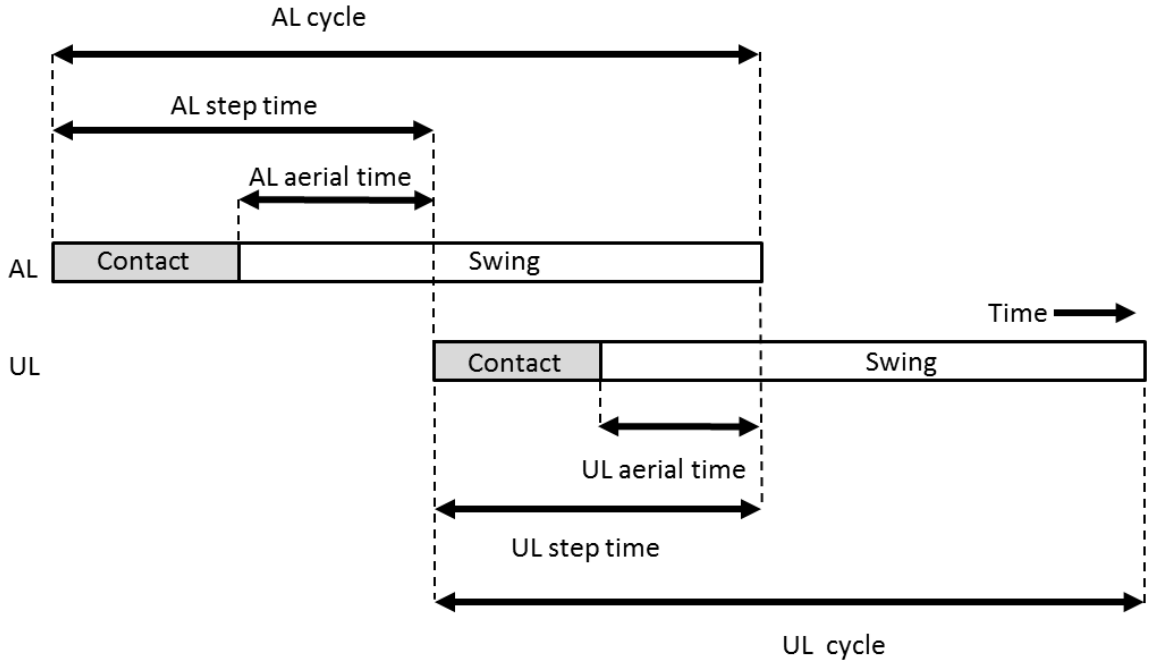

Figure 5.5 - Asymmetric running gait of a sprinter with a unilateral amputation. Although the affected leg (AL) and unaffected leg (UL) have identical cycle durations, they are 191° out of phase. The AL contact occurs earlier than the UL contact; thus AL step time is longer than UL step time.

5.5 Discussion

5.5.1 Straight vs. curve running

As hypothesized, all sprinters were slower during maximal sprint curve running compared to maximal sprint straight running. All athletes reported that they felt "uncomfortable" during clockwise curve running. However, every sprinter was able to perform each sprint without stumbling, slipping or any difficulty.

We measured curve running velocities of non-amputees that were well in accord with Greene's formula:

$$\left(\frac{v}{v_o}\right) \cong 1 - \frac{1}{2}\left(\frac{{v_o}^2}{Rg}\right)^2 \qquad (5.2)$$

where v is the maximum curve running velocity, v_o is the maximum straight running velocity, R is the curve radius (17.2 m in our experiment) and g is the acceleration due to gravity (Greene, 1985). For non-amputees, the difference between measured and predicted v for counterclockwise curve running was only -0.5% on average, and for clockwise curve running was -2.3% (Fig. 5.6 left panel). For non-amputees, we found no statistical difference in velocity between the two curve running directions (p=0.07), although this could be due to our small sample size. Five of the six non-amputees ran faster in the counterclockwise direction but the mean difference was only 1.9%.

For sprinters with leg amputations, we found that during curve running with the affected leg on the inside of the curve, velocities averaged 5.1% slower compared to curve running with the affected leg on the outside of the curve. This confirms our second hypothesis, that the maximum running velocity on curves of athletes with a unilateral leg amputation would be slower with their affected leg on the inside of the curve. Greene's formula overestimates curve running velocity with the affected leg on the inside of the curve, while it underestimates curve running velocity with the

affected leg on the outside of the curve: the difference between measured and predicted velocities being -4.0% and +3.2% , respectively (Fig. 5.6, right panel).

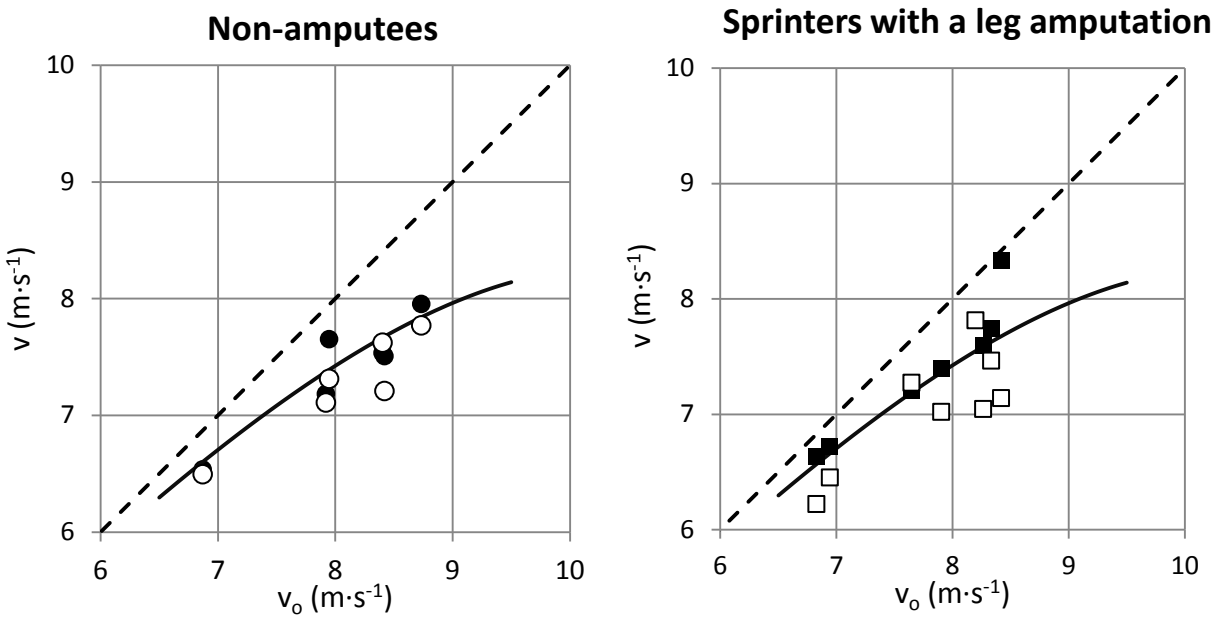

Figure 5.6 - Average maximum velocity during curve running (v) as a function of maximum velocity during straight running (v_o). The dashed line is the line of identity and the solid line is derived from Greene's equation (Greene, 1985). The velocities reported for counterclockwise curves (●) and clockwise curves (○) from non-amputees are slower than straight running velocities and are well-predicted by Greene's equation. Greene's equation underestimates velocity for sprinters with a leg amputation during curve running with the affected leg on the outside (■) and overestimates velocity during curve running with the affected leg on the inside (□).

During curve running, non-amputees and athletes with amputations spent more time on the ground with the inside leg compared to the outside leg. Our contact time measurements were in accord with those of previous studies (Ryan and Harrison 2003, Chang and Kram 2007). Although we did not perform ground reaction force measurements, previous studies allow some inference. Data from athletes with unilateral leg amputations sprinting straight ahead on a force-measuring treadmill (Grabowski et al. 2010) clearly indicate that the ground reaction forces generated by the affected leg are significantly lower compared to those of the unaffected leg. Data from non-amputees sprinting on curves (Chang and Kram, 2007) suggest that the ground reaction force generated by the leg on the inside of the curve limits curve running speed. Combining those two findings, we infer that the sprinting performance of the athletes with amputations was most impaired by their ability to generate force with their affected leg when it was on the inside of the curve.

The difference in step lengths between inside/outside legs of our sprinters during curve running was dissimilar to that of Chang and Kram (2007). They reported that the step lengths of the inside leg were significantly shorter than the step lengths of the outside leg during curve running. In the present study, we found that the step lengths of the inside leg of non-amputees were numerically longer compared to the step lengths of the outside leg in both curve running directions, but the difference was not statistically significant. The step lengths of both legs of athletes with amputations were the same during curve running with their affected leg on the outside of the curve. Although the mechanism is unclear, the difference between the results of our study and those of Chang and Kram (2007) could be due to the bigger curve radius (17.2 m) used in our study, compared to Chang and Kram (2007) experiments (6 m or less). Another difference between the two studies

is that our subjects were all trained sprinters, unlike the subjects in Chang and Kram (2007).

We have not made absolute statistical comparisons between non-amputees and athletes with amputations because they differ in personal best performances. The 100m personal records of athletes with amputations were 0.6 s (5%) slower, on average, than the 100m personal records of non-amputees; a large time difference in sprint performance. In addition, it is not yet possible to calculate the straight running speed reduction caused by an individual having a unilateral leg amputation, compared to that individual having two fully biological legs. During curves with the affected leg on the outside of the curve, athletes with amputations are limited by their unaffected (inside) leg, just like non-amputees. During straight running and curves with the affected leg on the inside of the curve, the affected leg limits overall performance.

5.5.2 Straight running: non-amputees vs. athletes with amputations

Despite the fact that individuals have a preferred (dominant) leg (Newton et al. 2006), all of our measurements on non-amputees showed symmetric left and right leg values during straight running trials. Non-amputee running gait can therefore be described as an alternating sequence of symmetric leg contact and swing times. Left and right leg cycle times (leg cycle time equals the time from foot contact to ipsilateral foot contact, it equals the sum of the contact and leg swing times of one leg, see Fig. 2) are almost perfectly out of phase (average phase difference was 182 degrees). In other words, foot contact of one leg occurs at nearly the middle of the contralateral leg cycle, resulting in equivalent left and right leg step lengths.

In contrast, the running gait of athletes with a leg amputation is not symmetric. Even during straight running trials, step times, and therefore step lengths, are longer for the affected leg compared to the unaffected leg. This results in a phase shift between the affected and unaffected legs (average phase difference was 191 degrees). The measured phase shift between affected and unaffected leg cycles means that athletes with amputations tend to initiate foot contact earlier with their affected leg, leading to longer step times and step lengths with the affected leg compared to unaffected leg (Fig. 3).

It must be noted that in both symmetric and asymmetric bipedal running, the leg cycle time of one leg must be equal, on average, to the leg cycle time of the other leg. If this rule were to be violated, a runner would need to take two steps in succession with the same leg after a certain number of steps. Athletes with amputations, who increase the contact time of their affected leg, must therefore decrease the leg swing time of their affected leg by the same amount, as is evident in our measurements (Tables 3 and 7) and also by a re-analysis of the data reported by Grabowski et al. (2010). Unlike our present data that show a 4% difference in leg

swing times between affected and unaffected legs during the straight running condition, Grabowski et al. (2010) reported no statistical difference between the affected and unaffected leg swing times of athletes with unilateral amputations during straight sprinting, although they acknowledged that their small number of subjects (n=6) may have limited their statistical power.

5.5.3 Limitations and Future Studies

We were only able to recruit two athletes with left leg amputations; therefore we could not perform statistical tests on this group alone. It must be noted, however, that all the measurements of the athletes with right leg amputations were consistent with those of the athletes with left leg amputations during curve running when legs were categorized as being on the inside versus on the outside of the curve. In addition, we measured the effects of only one curve radius, whereas different radii could provide more insight into the effects of curve running in sprinters with amputations. In the future, measurements of ground reaction forces during curve running in athletes with leg amputations would be useful for testing the inference of a force-deficit in the affected leg. In addition, measurements of leg stiffness and of ankle eversion and inversion or torsional stiffness at the "ankle level" of running specific prostheses during curve running trials could improve our understanding of the biomechanics of subjects with amputations, and of non-amputees.

5.6 Conclusions

As expected, non-amputees and athletes with amputations ran slower on curves, compared to straight running trials. Non-amputees velocities were similar on clockwise and counterclockwise curves. Athletes with amputations were slower on curves with the affected leg on the inside, compared to curves with the affected leg on the outside.

5.6 References

Chang YH, Kram R. Limitations to maximum running speed on flat curves. *J Exp Biol.* 210(6):971-82, 2007

Farley CT, Glasheen J, McMahon TA. Running springs: speed and animal size. *J Exp Biol.* 185(1), 71-86, 1993

Ferro A, Floria P. Differences in 200 m sprint running performance between outdoor and indoor venues. Journal of Strength and Conditioning Research 27(1):83-8. doi: 10.1519/JSC.0b013e31824f21c6, 2013

Greene PR. Running on flat turns: experiments, theory, and applications. *J Biomech Eng.* 107(2):96-103, 1985

Greene PR. Sprinting with banked turns. *J Biomech.* 20(7), 667-680, 1987

Grabowski AM, McGowan CP, McDermott WJ, Beale MT, Kram R, Herr HM. Running-specific prostheses limit ground-force during sprinting. *Biol Lett.* 23;6(2):201-4, 2010

Luo G, Stefanyshyn D. Limb force and non-sagittal plane joint moments during maximum-effort curve sprint running in humans. *J Exp Biol*. 215(Pt 24):4314-21. doi: 10.1242/jeb.073833. Epub 2012 Sep 12

IAAF Track and Field Facilities Manual, 2008 (http://www.iaaf.org)

Ker RF, Bennett MB, Bibby SR, Kester RC, Alexander RM. The spring in the arch of the human foot. *Nature*. 325(7000):147-9, 1987

Morton RH. Focus on Sport Statistical effects of lane allocation on times in running races *Statistician.* 46(1):101-104, 1997

Newton RU, Gerber A, Nimphius S, Shim JK, Doan BK, Robertson M, Pearson DR, Craig BW, Häkkinen K, Kraemer WJ. Determination of functional strength imbalance of the lower extremities. *J Strength Cond Res.* 20(4):971-7, 2006

Ryan GJ, Harrison AJ. Technical adaptations of competitive sprinters induced by bend running. *New Studies in Athletics*, 18(4), 57-70, 2003

Usherwood JR, Wilson AM. Accounting for elite indoor 200 m sprint results. *Biol Lett.* 22;2(1):47-50, 2006

6 Conclusions

A fundamental ability of all living creatures is the ability to respond to stimuli and to adapt to new conditions. The purpose of this research was to understand how different body characteristics, in particular different body masses and the use of running specific prostheses, influence the energetics and biomechanics of running.

In chapter 3 we measured the energy cost and the mechanical work of lean and obese subjects while they were running at constant speed. We found that mass-specific energy cost and mechanical work are independent of body mass. As a consequence, also efficiency is independent of body mass. The results strongly suggest that the elastic tissues of obese subjects can adapt (e.g., thickening) to the increased mass of the body thus maintaining their ability to store elastic energy, at the same level as the normal-weighted subjects.

In chapter 4 we analyzed the effect of starting block configuration on starting performance of both non-amputee sprinters and athletes with unilateral transtibial amputations. We found that the combination of both the resultant force and push angle determines horizontal force and therefore acceleration. We used single-leg measurements from unilateral amputees to simulate virtual non-amputees and virtual bilateral amputees. The results support the impression that, among similar-level athletes, bilateral amputees have slower starts than unilateral amputees, and unilateral amputees have slower starts than non-amputees.

In chapter 5 we compared curve running performance between non-amputee sprinters and sprinters with unilateral transtibial amputations. Both groups were slower during curves compared to straight running trials. Athletes with amputations were slower in curves with the affected leg on the inside, confirming the hypothesis that the limiting factor in curve running performance is the inside leg. Athletes with amputations tend to compensate the force impairment of the affected leg increasing

its contact time and also shifting the leg cycle phase, developing an asymmetric running gait, compared to non-amputees sprinters.

7 List of publications

7.1 Papers

Taboga P, Lazzer S, Fessehatsion R, Agosti F, Sartorio A, di Prampero PE. Energetics and mechanics of running men: the influence of body mass. *European Journal of Applied Physiology*, 112:4027-4033 2012

Taboga P, Marcolin F, Bordignon M, Antonutto G. Definition and validation of a comfort index calculation method for office seats. *La Medicina del Lavoro,* 103(1):58-67 2012

7.2 Conference proceedings

Taboga P, Lazzer S, Fessehatsion R, Agosti F, Sartorio A, di Prampero PE. Energetics and mechanics of running: the influence of body mass and obesity. Presentation at the 2012 Rocky Mountain Regional American Society of Biomechanics Meeting. April 21st, 2012 Boise (USA)

Acknowledgements

I would like to thank all the people who accompanied me throughout this journey. I apologize to those I forgot to mention.

Prof. Pietro Enrico di Prampero, you led me into a fascinating world. The more I walk or run into it, the more new "land, water and air" I see.

Prof. Guglielmo Antonutto, Dr. Stefano Lazzer, Dr. Enrico Rejc and Dr. Desy Salvadego, working with you helped my professional growth and critical thinking.

Gaetano, Davide and Marco, talking with you made me think "out of the box".

All the people of the Department of Medical and Biological Sciences, it was a pleasure to work with you.

All the volunteers who participated in the "cost of transport vs. mass" measurements and the staff of the Italian Institute for Auxology, Piancavallo (VB).

All the students of the School of Sports Sciences - University of Udine.

Prof. Rodger Kram, you taught me that science is made of good ideas, concrete work and having fun. Your support during and after my stay in Boulder was wonderful.

Dr. Alena Grabowski, for your help with the measurements, the writing, the housing and... the cookies!

Eileen and Vega, I felt at home with you. A piece of my heart is in Boulder.

Linda, Helen, Megan, Jason, Rich, Mickey, Reese and all the people I met at the Department of Integrative Physiology - University of Colorado at Boulder (USA).

The athletes who participated in the sprint running tests, you all deserve a gold medal.

The CU athletics department and track & field program for allowing us to use the Balch Fieldhouse indoor track facility.

Cathy Sellers of U.S. Paralympics Track and Field for help with recruiting athletes and for financial support for their travel.

Dr. Esteban Pavan, for being my external reviewer.

Gianni, my father, you taught me to think with my own mind.

Manuela, my mother, you are the background music of my life.

Marco, my brother, for being always at my side.

Aras, my four legged brother, you are pure joy.